Penerbit Akademia Baru

Journal of Advanced Research in Applied Mechanics
ISSN (online): 2289-7895 | Vol. 22, No. 1. Pages 13-48, 2016

A Review on Nonlinear Finite Element Analysis of Reinforced Concrete Beams Retrofitted with Fiber Reinforced Polymers

M. Kh. Hind[*,a], *M. Özakça*[b] *and T. Ekmekyapar*[c]

Department of Civil Engineering, University of Gaziantep, 27310 Gaziantep, Turkey
[*,a]*hindmahmood18@gmail.com*, [b]*ozakca@gantep.edu.tr*, [c]*ekmekyapar@gantep.edu.tr*

Abstract - *Fiber reinforced polymers materials have a wide use in a variety of applications, which are produced with a range of different stiffness and strength characteristics. However, these materials share identical orthotropic properties and ductility. In contrast, the ordinary concrete is isotropic and brittle material. This review study provides an efficient and simple three-dimensional frame finite element that able to estimate accurately the load-carrying capacity and deflection of reinforced concrete (RC) beams strengthened with fiber reinforced polymer (FRP) strips, plates or rods. In the context of a force base formulation (FB), which referred as fiber reinforced polymer force based beam, the proposed finite element considers distributed plasticity with the individual layer of the cross sections. Hundred seventy-six different specimen of retrofitted reinforced concrete beams have been included in the experimental database and numerical simulation in this study. These beams elements can model the collapse due to crush of concrete, reinforcing steel yielding, rod pull out, FRP rupture, diagonal shear, FRP debonding and cover separation. Three and four point bending loading tests were used to predict the load-carrying capacity and the deflection response of reinforced concrete beams. Based on several researches, experimental measurements and numerical simulations are compared according to different collected data. The numerical simulation results have a good agreement with the corresponding experimental results. From the statistical analysis study, it was found that the concrete strength is the most influential factor on the shear strength of the reinforced beams strengthened by FRP in the case of U-jacketing anchorage system. Where, the shear strength increased by 10.5%, 8.6% for tensile rupture and debonding failures, respectively, with increases in concrete strength. As a result, the simplicity, available requirements and computational efficiency of finite element simulation are the main advantages for using this analysis in various applications.* ***Copyright © 2016 Penerbit Akademia Baru - All rights reserved.***

Keywords: Nonlinear analysis, Finite element modeling, Reinforced concrete beams, Fiber reinforced polymers.

1.0 INTRODUCTION

The history of the concrete began since cement was introduced. It is generally used material in structural engineering everywhere throughout the world. Unreinforced concrete was a brittle material, with a low tensile strength and a low strain capacity. A revolutionary enhancement of concrete characteristics was employing steel bar reinforcement, which

Journal of Advanced Research in Applied Mechanics
ISSN (online): 2289-7895 | Vol. 22, No. 1. Pages 13-48, 2016

allows for the tensile forces to appear. Reinforced concrete turned into an effective option to other materials that were utilized as a part of bending elements. To increase compressive strength of the concrete, scientists worked intensively by discovering appropriate methods for consolidate the concrete. They have found that to implement economic designs, self-weight of structural elements and their dimensions can reduce. As a consequence of these rigorous studies, employing high-strength concrete elements came to be a common trend in developed constructions. Since Babylonian and Egyptian civilizations, Fibers were used to strengthen brittle materials before cement was known, as discussed by Nawy [1]. Mohammadi et al. observed that in order to increase the strain at peak load, and provide a supplementary energy absorption ability of RC elements and structures, fibers were used. They recently identified that the fibers significantly enhance static flexural strength of concrete as well as its impact strength, tensile strength, ductility and flexural toughness leading to increase the concrete elements ductility [2].

Fiber reinforcement is typically randomly distributed over the whole element. Furthermore, it can be used in a portion of the element's section, for instance, in composite elements such as two-layer beams or in high-strength concrete columns, covered by fiber reinforced concrete. [2-4]. During the past nine decades, several types of fibers have been used on a large scale to improve performance of concrete, such as steel, textile, organic and glass [5].

Heinzle indicated that fibers design is influenced by different parameters such as fiber's content and geometry, bond strength between fiber and binder matrix, strength of the matrix, shrinkage of the concrete orientation of fibers. Therefore, a very methodical vision concerning the tensile carrying behavior of fibered concrete is required [6]. Effectiveness of fibers added to concrete can be achieved practically or numerically. The routine laboratory testing methods are impact test, compressive test, tensile and flexural tests [7].

The influence of fibers on the concrete properties and performance such as strength, toughness, ductility, post cracking load resistance and durability has been taken into account in several studies [8, 9]. Where the effect of the various types of fibers was observed experimentally by authors through using different kinds of concrete [10-12]. To assess the fiber orientation and its effect on the flexural strength, the researchers analyzed the effect of aggregate and fiber-reinforced concrete production cost in addition to its mechanical properties [13, 14].

During the last decades, the use of fiber reinforced concrete has constantly increased in civil engineering applications due to the high particular stiffness and specific strength. It is currently applied in fields such as highway and airport pavements, earthquake-resistant structures, bridges, tunnels and hydraulic structures [15-17]. The main purpose of using the fibers is to strengthen the reinforced concrete constructions [18]. Consequently, studies have been conducted on the FRP or polymer strengthened reinforced concrete (RC) beams, columns and slabs, as well as masonry and concrete walls [19].

Civil engineering structures have been strengthened by using fiber-reinforced polymer (FRP) widely [20-24]. Hawileh et al. gave a comprehensive review on Externally Bonded Reinforcement technique (EBR), which is one of the most common applications to strength the reinforced concrete (RC) members by bonding externally FRP laminates or sheets with epoxy [25]. Recently, the alternative technique has been getting high attention named Near

Penerbit
Akademia Baru

Journal of Advanced Research in Applied Mechanics
ISSN (online): 2289-7895 | Vol. 22, No. 1. Pages 13-48, 2016

Surface Mounted (NSM) technique. This technique involving an inserted FRP material into slits pre-cut in the concrete cover [26, 27]. The higher bonding area and the confinement which offered by NSM technique in a better anchoring capacity provide more efficiency than EBR technique [28-30].

As shown in Figure 1, there are four main types of failure mode for reinforced concrete beams retrofitted with FRP layers. They can be identified as follows: (1) flexure failure, (2) FRP rupture failure mode, (3) debonding failure mode (divided into four modes, end debonding, intermediate debonding caused by flexural cracks, debonding caused by diagonal cracks, debonding caused by irregularities and roughness of concrete surface, see Figure 2), and (4) shear failure. In addition, there are five possible failure modes for single or double shear tests, which are: concrete crushing, plate tensile failure including FRP rupture or steel yielding, adhesive failure, concrete-to-adhesive interfacial failure and plate-to-adhesive interfacial failure. For more detail on failure modes see [31-34].

This article presents an exhaustive review of nonlinear finite element studies for FRP retrofitted reinforced concrete beams and suggests a direction for future developments. In addition, this review interested in four main points, (1) study the different types of analytical models, considering the achievement of accuracy for practical applications, (2) explore the most factor effect on the shear strength of reinforced concrete beams retrofitted with FRP, (3) examine the common failure mode that appears in the retrofitted RC beams and describes their performance, and (4) reduce the computational cost and complexity of finite element analysis method.

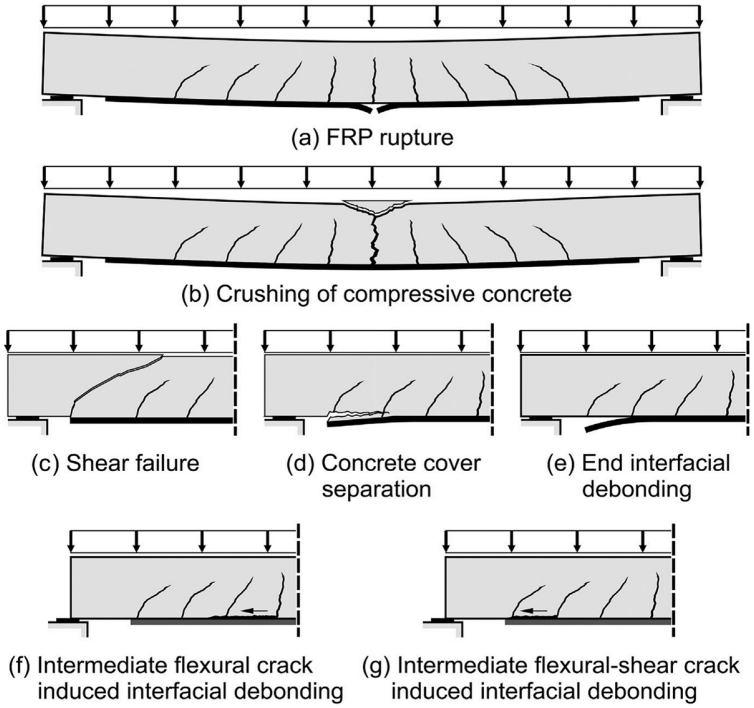

Figure 1: Failure modes of RC beams strengthened with FRP [35]

Penerbit Akademia Baru
Journal of Advanced Research in Applied Mechanics
ISSN (online): 2289-7895 | Vol. 22, No. 1. Pages 13-48, 2016

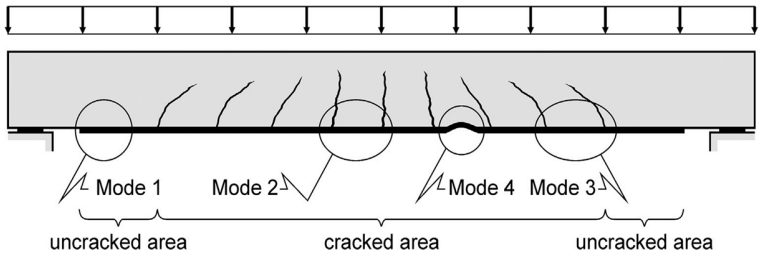

Figure 2: Debonding failure modes of RC beams strengthened with FRP [4]

2.0 FINITE ELEMENT ANALYSIS

The behavior of reinforced concrete beams is investigated by experimental studies extensively. The beams theoretical calculations of deflections and internal stress/strain distributions are compared with the experimental results. In order to provide a valuable supplement to the laboratory tests especially in parametric studies, finite element analysis (FEA) can be used to model the behavior of beams numerically. It appears from the aforementioned researches that finite element analysis which utilized in structural engineering, estimates the overall behavior of a structure through dividing it into a number of simple elements, each one of them has well-defined mechanical and physical characteristics.

Nilson et al. mentioned that the biggest challenge in the finite element analysis of civil engineering structures is modeling the complex behavior of reinforced concrete whether non homogeneous or anisotropic properties. The effects of cracking based on a pre-determined crack patterns are adopted in more recent finite element models of reinforced concrete [36-39]. Furthermore, the topology adjustments of the models were needed such as the incremental load; consequently, the ease and speed of the analysis were limited [40].

In representation of the cracked concrete as an orthotropic material, a smeared cracking methodology was introduced using isoperimetric formulations as Rashid et al. suggestions [41]. When the principal tensile stress exceeds the ultimate tensile strength, cracking of the concrete occurs. In contrast, in the direction parallel to the principal tensile stress direction, the elastic modulus of the material is assumed to be zero [42-53].

Recently using the finite element method, the researchers tried to simulate the behavior of reinforced concrete strengthened with FRP composites. The smeared cracking approach was used to model the behavior and failure mechanisms of those experimental beams which were tested in the laboratory [46, 54-67].

However, there have been no controlled studies, which compare differences in using nonlinear finite element analysis programs. Each program has its own designation, analysis procedures and different elements that need to be used correctly. On the other hand, to keep up with new technologies, the designer / analyst must be completely acquainted with the finite element tools [68]. This research has been covered the studies which conducted using the ANSYS program, where element's modeling and properties described in the following sections.

Penerbit Akademia Baru

Journal of Advanced Research in Applied Mechanics
ISSN (online): 2289-7895 | Vol. 22, No. 1. Pages 13-48, 2016

2.1 Elements Type and Characteristics for FE Models

2.1.1 Concrete Modeling

As reported by ANSYS user's guide, Solid65 an eight-node solid element was utilized to model the concrete. The element is capable of plastic deformation, cracking in three orthogonal directions, and crushing. The solid element has eight nodes with three degrees of freedom at each node translations in the nodal x, y, and z directions [68]. The geometry for this element type is illustrated in Figure 3.

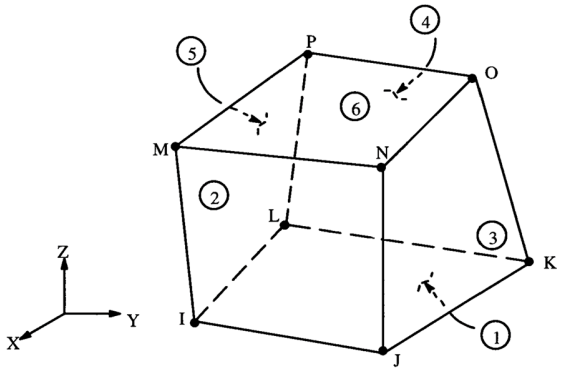

Figure 3: Solid65 – 3D reinforced concrete solid [68]

Shah et al. noted that the concrete has different behavior in compression and tension. This is due to being quasi-brittle material, which has tensile strength between 8-15% of the compressive strength. Therefore, the development of a model for the behavior of concrete is a difficult task [69]. Figure 4 clarifies a typical stress-strain curve for concrete.

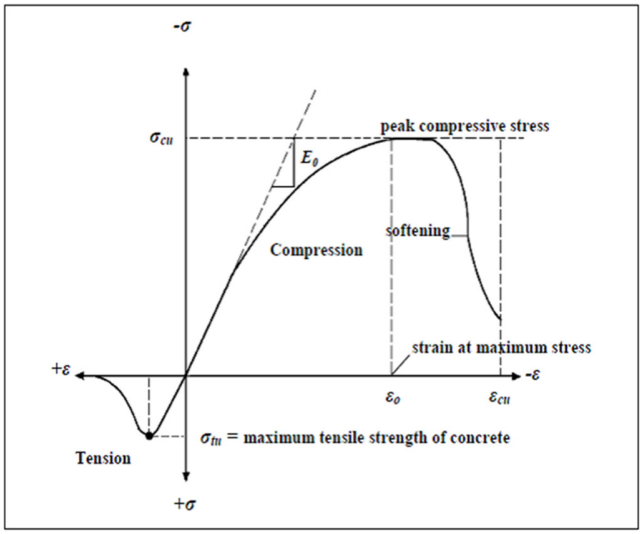

Figure 4: Typical stress-strain curve for concrete [45]

As mentioned by Barbosa et al. "In compression, the stress-strain curve for concrete is linearly elastic up to about 30 percent of the maximum compressive strength. Above this

Journal of Advanced Research in Applied Mechanics
ISSN (online): 2289-7895 | Vol. 22, No. 1. Pages 13-48, 2016

point, the stress increases gradually up to the maximum compressive strength. After it reaches the maximum compressive strength σ_{cu} , the curve descends into a softening region, and eventually crushing failure occurs at an ultimate strain ε_{cu}" [70, 71]. Georgin et al. identified that "The stress-strain curve for concrete is approximately linearly elastic up to the maximum tensile strength in tension. After this point, the concrete cracks and the strength decreases gradually to zero" [45, 72-74].

ANSYS requires input data for concrete are:

- Modulus of elasticity (*Ec*).
- Ultimate uniaxial compressive strength ($f_c^{'}$).
- Ultimate uniaxial tensile strength (*ft*).
- Poisson's ratio (v).
- Shear transfer coefficient (βt).
- Compressive uniaxial stress-strain relationship for concrete.

To estimate the actual elastic modulus of the beams, an effort was made using the ultrasonic pulse velocity method [75-77]. The ultimate concrete compressive and tensile strengths for each beam model were calculated by Equations 1 and 2, respectively [78].

$$f_c^{'} = \left(\frac{E_c}{57000}\right)^2 \tag{1}$$

$$f_t = 7.5\sqrt{f_c^{'}} \tag{2}$$

Where: E_c, $f_c^{'}$ and f_t are in psi.

The shear transfer coefficient, βt, represents conditions of the crack face. The value of βt ranges from 0.0 to 1.0, with 0.0 representing a smooth crack (complete loss of shear transfer) and 1.0 representing a rough crack (no loss of shear transfer) [68, 79]. The value of βt used in many studies of reinforced concrete structures varied between 0.05 and 0.25 [35, 45, 46].

In order to create uniaxial compressive stress-strain curve for concrete, Equations 3, 4 and 5 are used as follows [80, 81]:

$$f = \frac{E_c \varepsilon}{1 + \left(\frac{\varepsilon}{\varepsilon_o}\right)^2} \tag{3}$$

$$\varepsilon_o = \frac{2 f_c^{'}}{E_c} \tag{4}$$

$$E_c = \frac{f}{\varepsilon} \tag{5}$$

Penerbit Akademia Baru

Journal of Advanced Research in Applied Mechanics
ISSN (online): 2289-7895 | Vol. 22, No. 1. Pages 13-48, 2016

Where:

f = stress at any strain ε

ε = strain at stress f

ε_o = strain at the ultimate compressive strength $f_c^{'}$

Figure 5 shows the simplified compressive uniaxial stress-strain relationship.

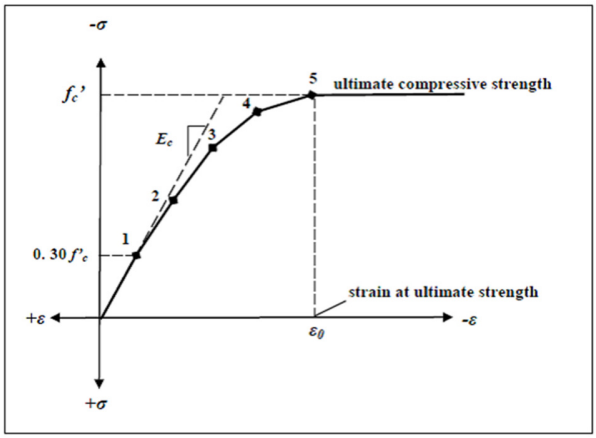

Figure 5: Simplified compressive uniaxial stress-strain curve for concrete [45]

Both cracking and crushing failure modes are accounted for concrete materials [82]. To define a failure surface for the concrete, ultimate tensile and compressive strengths are needed [83, 84]. Figure 6 illustrates the three-dimensional failure surface for concrete. Dahmani et al. explained that "The most significant nonzero principal stresses are in the x and y directions, represented by σ_{xp} and σ_{yp}, respectively. Three failure surfaces are shown as projections on the σ_{xp}-σ_{yp} plane. The mode of failure is a function of the sign of σ_{zp} (principal stress in the z direction)" [85-87].

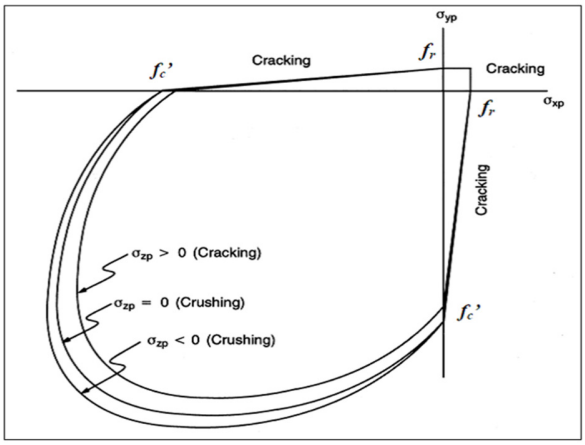

Figure 6: 3D failure surface for concrete [68]

Penerbit
Akademia Baru

Journal of Advanced Research in Applied Mechanics
ISSN (online): 2289-7895 | Vol. 22, No. 1. Pages 13-48, 2016

Researchers found that when the principal tensile stress in any direction lies outside the failure surface, cracking occurs in a concrete element. In the direction parallel to the principal tensile stress direction, the elastic modulus of the concrete element is set to zero after cracking [36, 88, 89]. When all principal stresses are compressive and lie outside the failure surface, crushing occurs. Thereafter, the elastic modulus is set to zero in all directions and the element effectively disappears. [68, 90].

According to Mindess et al., crack's formation and thus concrete failure attributed to the weakness of concrete in tension. Where the specimen is subject to a uniaxial compressive load in compression test. Secondary tensile strains caused by the impact of Poisson occur perpendicular to the load [69, 91, 92].

2.1.2 Steel Reinforcement Modeling

To model the steel reinforcement a Link8 element was used as described by ANSYS user's guide. The element is capable of plastic deformation, where two nodes are required for this element. Each node has three degrees of freedom translations in the nodal x, y, and z directions [93]. The geometry for this element type is illustrated in Figure 7.

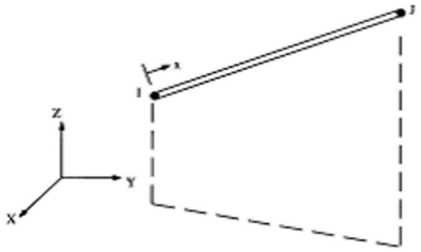

Figure 7: Link8 – 3D spar [68]

For the finite element models, the reinforced steel was identical in tension and compression and assumed to be an elastic-perfectly plastic material [94, 95]. ANSYS input data requirements for reinforced steel are:

- Modulus of elasticity (E_s).
- Yield stress (f_y)
- Poisson's ratio (v)

Figure 8 shows the stress-strain relationship for the steel reinforcement.

However, it was later shown by several studies that to provide the perfect bond between the concrete and steel reinforcement, the two materials should share the same nodes by using link element connecting between nodes of each adjacent concrete solid element.

Penerbit
Akademia Baru

Journal of Advanced Research in Applied Mechanics
ISSN (online): 2289-7895 | Vol. 22, No. 1. Pages 13-48, 2016

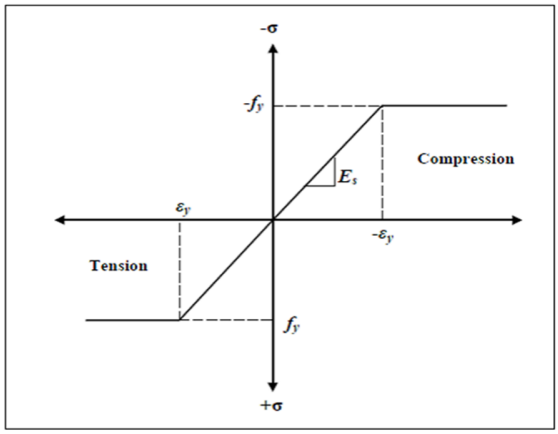

Figure 8: Stress-strain curve for steel reinforcement [68]

2.1.3 Steel Plates Modeling

Solid45 was used for the steel plate's modeling in the beam at the supports and loading location as proposed by Mostofinejad et al. The element is identified with eight nodes having three degrees of freedom at each node translation in the nodal *x*, *y*, and *z* directions [96]. The geometry for this element type is clarified in Figure 9.

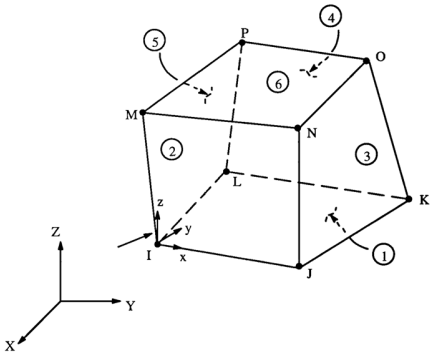

Figure 9: Solid45 – 3D solid [68]

In the finite element models to provide a more even stress distribution over the support areas, steel plates were added at support and loading locations as in the actual beams. ANSYS input data requirements for steel plate are:

- Elastic modulus (E_s)
- Poisson's ratio (v)

2.1.4 FRP Composites Modeling

According to ANSYS user's guide, Solid46 a layered solid element was utilized to model the FRP composites. The element has three degrees of freedom at each node and translations in the nodal *x*, *y*, and *z* directions. Furthermore, the element allows for up to 100 different material layers with different orientations and orthotropic material properties in each layer [68]. The geometry for the solid46 is illustrated in Figure 10.

Penerbit Akademia Baru

Journal of Advanced Research in Applied Mechanics
ISSN (online): 2289-7895 | Vol. 22, No. 1. Pages 13-48, 2016

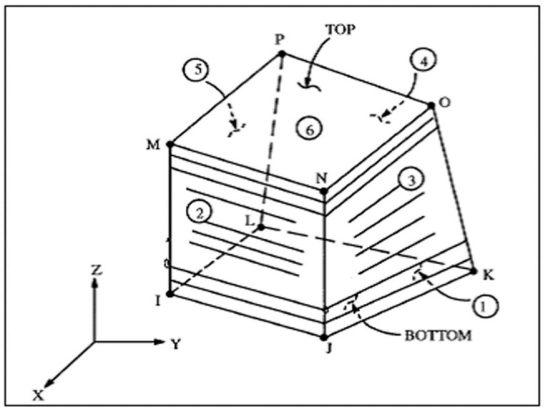

Figure 10: Solid46 – 3D layered structural solid [68]

FRP composites can be defined as materials that consist of two constituents. One constituent is the reinforcement, and the second constituent is a continuous polymer called the matrix. These constituents are combined at a macroscopic level and are not soluble in each other [97]. The FRP composites are anisotropic materials which their properties are different in all directions. Carbon and glass represent the reinforcing material in the form of fibers. The reinforcing materials are usually stiffer and stronger than the matrix. Figure 11 shows a schematic of FRP composites.

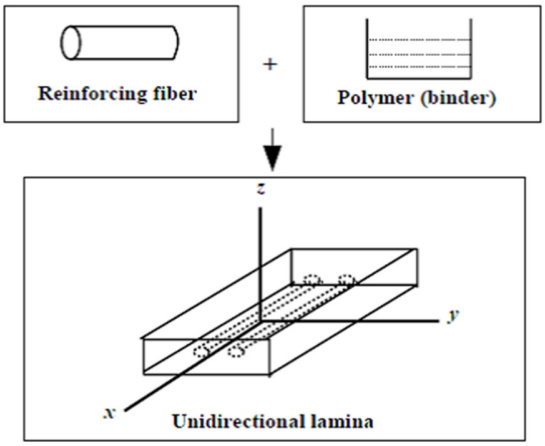

Figure 11: Schematic of FRP composites [97, 98]

The unidirectional layer has three mutually orthogonal planes of material characteristics (xy, xz, and yz planes) as displayed in Figure 11. The xyz coordinate axes represent the principal material coordinates [98, 99].

ANSYS input data requirements for the FRP composites are as follows:

- Number of layers.
- Thickness of each layer.
- Orientation of the fiber direction for each layer.
- Elastic modulus of the FRP composite in three directions (E_x, E_y and E_z).

Journal of Advanced Research in Applied Mechanics
ISSN (online): 2289-7895 | Vol. 22, No. 1. Pages 13-48, 2016

- Shear modulus of the FRP composite for three planes (G_{xy}, G_{yz} and G_{xz}).
- Major Poisson's ratio for three planes (v_{xy}, v_{yz} and v_{xz}).

The properties of isotropic materials are identical in all directions such as elastic modulus and Poisson's ratio. Nevertheless, this is not the case with orthotropic materials. E_x is the modulus of elasticity in the fiber direction. E_y is the modulus of elasticity in the y direction perpendicular to the fiber direction. That's mean $E_x \neq E_y$ and $v_{xy} \neq v_{yx}$ [100, 101]. For the ANSYS program the orthotropic material data are provided in the v_{xy} or major Poisson's ratio format. The major Poisson's ratio is the ratio of strain in the y direction to strain in the perpendicular x direction when the applied stress is in the x direction. The quantity v_{yx} is called a minor Poisson's ratio and is smaller than v_{xy}, while E_x is larger than E_y. Equation 6 clarifies the relationship between v_{xy} and v_{yx} [102].

$$v_{yx} = \frac{E_y}{E_x} v_{xy} \tag{6}$$

Where:

v_{yx} : Minor Poisson's ratio

E_x : Modulus of elasticity in the x direction (fiber direction)

E_y : Modulus of elasticity in the y direction

v_{xy} : Major Poisson's ratio

2.2 Finite Element Discretization, Loading and Boundary Condition

The mesh terms refer to a division of the model into small elements. In this case, after applied loads, stress and strain are computed at intersection nodes of these small elements [103]. When an appropriate number of elements utilized in the model, a convergence of results will be obtained. Therefore, selection of the mesh density is an important step in finite element modeling [104]. The researchers suggested that the number of concrete elements for the whole reinforced beam should be at least 6000 elements [105]. In accordance with most studies, rectangular mesh is recommended for Solid65 (concrete) element. The individual elements are created in the modeling of steel reinforcing through the concrete nodes; that means no mesh is required for the reinforcement bar [106].

2.3 Nonlinear Solution

The total load applied to a finite element model is divided into a series of load increasing progressively called steps of load. Newton- Raphson equilibrium iteration was one of the options for ANSYS program, which uses this approach for updating the model stiffness [107, 108]. Figure 12 illustrates the use of the Newton-Raphson approach.

Journal of Advanced Research in Applied Mechanics
ISSN (online): 2289-7895 | Vol. 22, No. 1. Pages 13-48, 2016

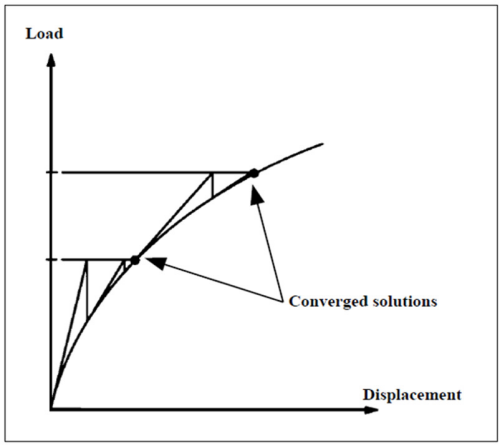

Figure 12: Newton-Raphson iterative solution [68]

Newton-Raphson approach assesses the difference between the loads corresponding to the element stresses and the applied loads. After that, the program implements a linear solution and checks for convergence. When convergence criteria are not satisfied, stiffness matrix is updated and a new solution is obtained. This iterative procedure continues until the problem converges [68, 109, 110].

The researchers suggested that to provide convergence at the end of each load increment, tolerance limits may range from 0.05 to 0.2 [111]. Automatic time stepping within ANSYS program controls load step sizes for the nonlinear analysis. The maximum and minimum load step sizes are required for the automatic time stepping.

3. Correlation between Numerical Simulation and Experimental Results

Correlation study was conducted in large-scale between experimental results and numerical simulations in accordance with the collected data in this paper. Hundred seventy six different specimen of reinforced concrete beams have been included in the experimental database and numerical simulation. These specimens divided into two groups: reference reinforced concrete beams without FRP laminates and reinforced concrete beams retrofitted with bonded FRP (strips, plates or rods). Twenty six different study [112 –137] and its available data have been gathered and analyzed statistically in this research. Interestingly, this correlation is related to the ultimate load-carrying capacity and deflection of simply supported reinforced concrete beams retrofitted with FRP. In addition, these beams are subjected to a 4-point bending test and 3-point bending test.

Among the plausible explanations for these findings is that assess the performance of finite element analysis and follow-up with new developments in the use of soft wares to achieve better results. Where, these results are confirmed by the comparison between the practically measurement and numerically prediction for load-carrying capacity and deflection for the beams. Table 1 presents both reference and retrofitted beams geometric properties, the used materials' mechanical properties and the corresponding anchorage systems. It is apparent from the collected studies that the test data and available information mostly obtained through steel coupon and FRP tensile tests or concrete compression tests. This table is quite revealing in several ways such as showing results with a wide range of lengths (from 1000

Journal of Advanced Research in Applied Mechanics
ISSN (online): 2289-7895 | Vol. 22, No. 1. Pages 13-48, 2016

mm to 6096 mm), cross-section widths (from 100 mm to 375 mm), cross-section heights (from 100 mm to 768.4 mm), concrete peak strength (from 13.02 MPa to 80 MPa), concrete modulus of elasticity (from 17.08 GPa to 41.3 GPa), steel reinforcement areas (from 51 mm^2 to 981.7 mm^2 in the tension side and from 0 mm^2 to 339 mm^2 in the compression side) and steel modulus of elasticity (from 183.6 GPa to 215GPa). A wide variation of FRP reinforcement configurations, with four materials (CFRP, GFRP, AFRP and SFRP) included in this study. Furthermore, four different anchorage systems were studied; (a) linear anchorage, which provided by the bonding between FRP and concrete through the adhesive layer, (b) U-wrap, which an FRP sheet is bonded at each plate end from one side to the other of the beam cross-section, (c) Bolts + U-wrap, which bolts are positioned at each FRP plate end in addition to the U-shaped FRP sheet, and (d) U-shape, which the FRP plate/sheet is bonded also on the sides of the reinforced concrete beam cross-section along the entire length of the FRP reinforcement.

Table 2 highlights the load-carrying capacities and deflection experimental measurement and numerical simulation values of retrofitted reinforced concrete beams. Besides that, it offers the ratio (P_{FE}/P_{EXP}, δ_{FE}/δ_{EXP}) and failure mode of beams. For the reference reinforced concrete beams the values of Mean and coefficient of variation (COV) were equal to 1.02, 0.07 for loads and 1.02, 0.11 for deflections, respectively. The statistical study shows that the simulation capabilities of the retrofitted beams elements are highly satisfactory in which, Mean = 0.99 and COV = 0.14 for loads and Mean = 1.06, COV = 0.25 for deflections. The maximum and minimum values of the ratios are 1.44 and 0.62 for loads, 2.51 and 0.53 for deflections, respectively.

The use of numerical simulation software showed that the failure modes were identical to the failure that displayed by each model when tested experimentally. That is an important development to study the types of failures that exposed structures theoretically and identify it by applying the finite element methods. In accordance with the reference beams it can be seen that the flexure failure is prevalent in which values of Mean and COV were 0.98, 0.03 for loads and for deflections the values were 1.14, 0.11, respectively. The single most striking observation to emerge from the data comparison was that the common failure mode for retrofitted beams is the cover separation failure (45 cases) with Mean and COV of 0.95, 0.19 for loads and 0.72, 0.31 for deflections, respectively.

Further clarification, the data in Table 2 which involve the loads and deflections for reference beams (without FRP) has been illustrated graphically as shown in Figures 13, 14. Where, the dashed line on the main diagonal has been plotted to refer to the perfect agreement between the experimental results and numerical simulations. On the other hand, it can be seen that most tests handled beams with load carrying capacity lower than 500 kN and deflection lower than 80 mm. The results of Table 2 have presented graphically regarding to the loads and deflections for FRP beams in Figures 15, 16. To represent the perfect agreement between the experimental results and numerical simulations, dashed line on the main diagonal has been placed. It can be observed that most tests handled beams with load carrying capacity lower than 600 kN and deflection lower than 95 mm.

Penerbit Akademia Baru
Journal of Advanced Research in Applied Mechanics
ISSN (online): 2289-7895 | Vol. 22, No. 1. Pages 13-48, 2016

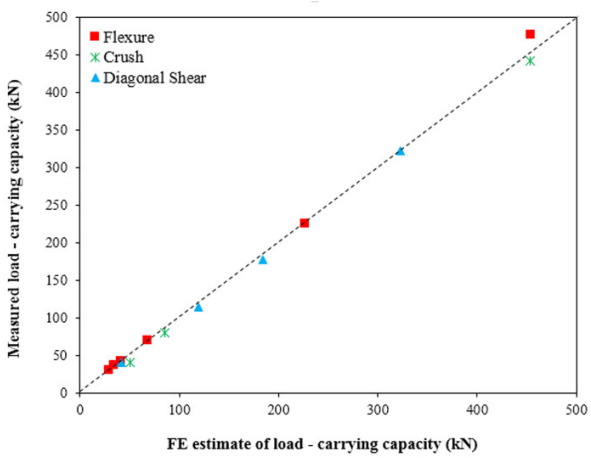

Figure 13: Comparison between experimental measurement and FE simulation of the ultimate load-carrying capacity for reference reinforced concrete beams

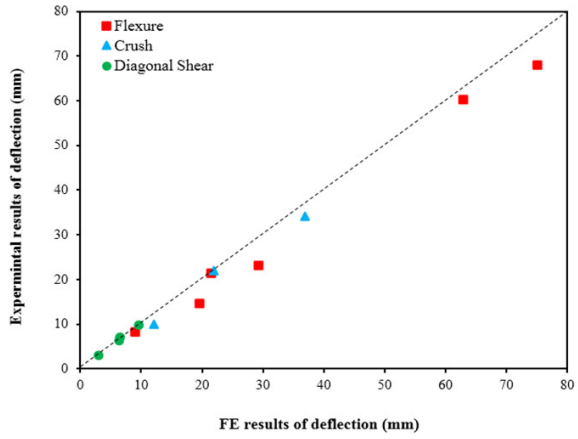

Figure 14: Comparison between experimental measurement and FE simulation of the deflection response for reference reinforced concrete beams

Consistent with findings, the data seem to show that the experimental measurement and finite element simulation of deflections are slightly less accurate than the results of the maximum applied force (ultimate load carrying capacity).

Penerbit Akademia Baru

Journal of Advanced Research in Applied Mechanics
ISSN (online): 2289-7895 | Vol. 22, No. 1. Pages 13-48, 2016

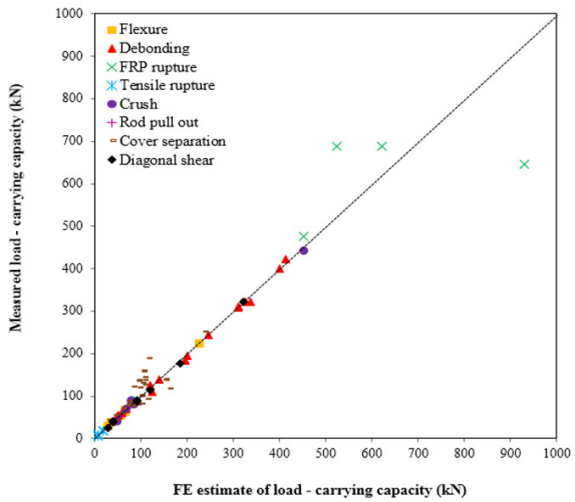

Figure 15: Comparison between experimental measurement and FE simulation of the ultimate load-carrying capacity for FRP reinforced concrete beams

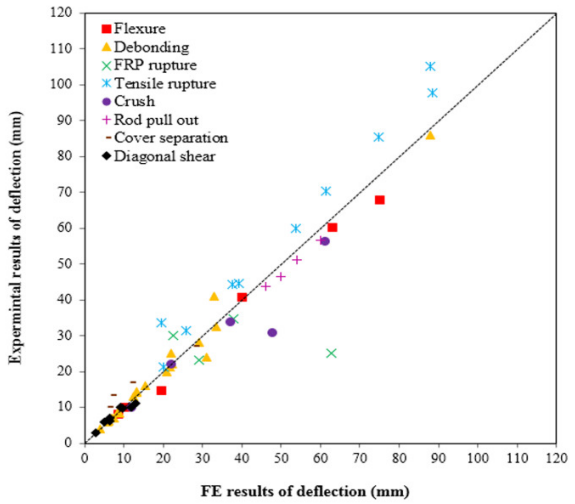

Figure 16: Comparison between experimental measurement and FE simulation of the deflection response for FRP reinforced concrete beams

It appears from the aforementioned investigations that numerous studies have been conducted the effects of strength the reinforced concrete beams by FRP in terms of different factors. The first important factor mentioned throughout this study is the beam width, in which beams with large width have a lower proportion of exposure to failure. That's meant that the failure transferred from the reinforced beam to the FRP layer. The shear strength of reinforced beams strengthened by side bonding of an FRP laminates increases by 3.6% and 2.2% for tensile rupture and debonding failures, respectively, with

Journal of Advanced Research in Applied Mechanics
ISSN (online): 2289-7895 | Vol. 22, No. 1. Pages 13-48, 2016

increasing in beam width, whilst in the case of U-jacketing, the shear strength increases by 4.1% and 3.2% for tensile rupture and debonding failures, respectively.

Second main factor is FRP thickness. With an increases in the thickness of FRP, the effective strain will be decrease, and the shear strength of the reinforced concrete beam will be increase. However, the same effect was observed on the failure modes for different anchorage system where the increase of shear strength was 8%.

The third important factor is strength of concrete. In accordance with the results provided in Table 2, the shear strength of reinforced beams strengthened by side bonding of an FRP layers increases by 7.1% and 5.8% for tensile rupture and debonding failures, respectively, with increasing in concrete strength, whilst in the case of U-jacketing, the shear strength increases by 10.5% and 8.6% for tensile rupture and debonding failures, respectively. It is noted that the effect of concrete strength on the probability of tensile rupture failure is greater than its effect on probability of debonding failure.

There are quite few research studies on the effect of FRP type, FRP height, the number of FRP layers and FRP modulus of elasticity on the concrete strength and durability. However, studies on these factors are rare to find in literature. Moreover, no attempt was done to explore the potential of using FRP composites for construction in severe environments. Additionally, far too little attention has been paid to study the anchorage system, and its huge complexity in modeling. Important issues relating to the new generations of FRP materials and the use of suitable numerical analysis modeling to verify their performance have to be studied more consistently in the future.

Table 1: Geometry and material properties of reinforced concrete beams retrofitted with FRP

Tests	L (mm)	b (mm)	h (mm)	$A_{y,bottom}$ (mm^2)	$A_{y,top}$ (mm^2)	E_c (GPa)	f_c (MPa)	f_t (MPa)	E_y (GPa)	f_y (MPa)	FRP Type	b_f (mm)	t_f (mm)	E_f (GPa)	No.of layers	Anchorage
Bennegadi,Sereir and Amziane [112]																
A	1500	100	160	157.08	100.53	29.545	39.1	3.95	200	550	----	----	----	----	----	None
B	1500	100	160	157.08	100.53	29.545	39.1	3.95	200	550	CFRP	100	2	27	1	FRP sheet
C	1500	100	160	157.08	100.53	29.545	39.1	3.95	200	550	CFRP	100	4	27	1	FRP sheet
D	1500	100	160	157.08	100.53	29.545	39.1	3.95	200	550	CFRP	100	6	27	1	FRP sheet
Ozcan, bayraktar, Sahin, Haktanir and Türker [113]																
A	2000	250	350	276.46	100.53	29.50	24.46	1.59	200	420	----	----	----	----	----	None
B	2000	250	350	----	----	27.50	22.48	1.52	----	----	SF	60	0.75	27.50	----	----
C	2000	250	350	----	----	26.50	21.80	1.49	----	----	SF	60	0.75	26.50	----	----
D	2000	250	350	----	----	26.50	21.34	1.48	----	----	SF	60	0.75	26.50	----	----
E	2000	250	350	----	----	26.50	22.59	1.52	----	----	SF	60	0.75	26.50	----	----
Jayajothi, Kumutha and Vijai [114]																
CB1	3200	125	250	226.19	157	----	----	----	----	----	----	----	----	----	----	None
FRP1	3200	125	250	226.19	157	----	----	----	----	----	CFRP	125	0.3	----	1	FRP sheet
CB2	3620	150	250	226.19	157	----	----	----	----	----	----	----	----	----	----	None
FRP2	3620	150	250	226.19	157	----	----	----	----	----	CFRP	150	0.3	----	1	FRP sheet
Kachlakev and Miller [115]																
A1	6096	305	768.4	115.45	76.18	19.35	16.71	2.546	200	410	----	----	----	----	----	None
B1	6096	305	768.4	115.45	76.18	17.55	13.75	2.309	200	410	CFRP	162.5	1.0	62	6	FRP sheet
C1	6096	305	768.4	115.45	76.18	18.16	14.73	2.390	200	410	GFRP	731.3	1.3	21	6	FRP sheet
D1	6096	305	768.4	115.45	76.18	17.08	13.02	2.247	200	410	C,GFRP	731.3	1.0,1.3	62,21	3,3	FRP sheet
Sayed,Wang and Wu [116]																
S-t1	2400	200	400	339.29	235.62	25.74	30	3.39	210	360	FRP	400	0.4	200	1	Bonding
S-t2	2400	200	400	339.29	235.62	25.74	30	3.39	210	360	FRP	400	0.5	200	1	Bonding
S-t3	2400	200	400	339.29	235.62	33.23	50	4.38	210	360	FRP	320	0.1	200	1	Bonding
S-t4	2400	200	400	339.29	235.62	33.23	50	4.38	210	360	FRP	320	0.2	200	1	Bonding
S-t5	2400	200	400	339.29	235.62	33.23	50	4.38	210	360	FRP	320	0.3	200	1	Bonding
S-E6	2400	200	400	339.29	235.62	25.74	30	3.39	210	360	FRP	400	0.2	165	1	Bonding
S-E7	2400	200	400	339.29	235.62	25.74	30	3.39	210	360	FRP	400	0.2	244	1	Bonding
S-E8	2400	200	400	339.29	235.62	25.74	30	3.39	210	360	FRP	400	0.1	165	1	Bonding
S-E9	2400	200	400	339.29	235.62	25.74	30	3.39	210	360	FRP	400	0.1	230	1	Bonding
S-E10	2400	200	400	339.29	235.62	25.74	30	3.39	210	360	FRP	400	0.1	244	1	Bonding
S-b11	2400	160	400	339.29	235.62	25.74	30	3.39	210	360	FRP	400	0.2	200	1	Bonding
S-b12	2400	240	400	339.29	235.62	25.74	30	3.39	210	360	FRP	400	0.2	200	1	Bonding
S-b13	2400	300	400	339.29	235.62	25.74	30	3.39	210	360	FRP	400	0.2	200	1	Bonding
S-b14	2400	360	400	339.29	235.62	25.74	30	3.39	210	360	FRP	400	0.2	200	1	Bonding
S-fc15	2400	200	400	339.29	235.62	21.02	20	2.77	210	360	FRP	400	0.2	200	1	Bonding
S-fc16	2400	200	400	339.29	235.62	23.50	25	3.10	210	360	FRP	400	0.2	200	1	Bonding
S-fc17	2400	200	400	339.29	235.62	29.73	40	3.92	210	360	FRP	400	0.2	200	1	Bonding
S-fc18	2400	200	400	339.29	235.62	23.50	25	3.10	210	360	FRP	400	0.1	200	1	Bonding

S-fc19	2400	200	400	339.29	235.62	29.73	40	3.92	210	360	FRP	400	0.1	200	1	Bonding
S-hf20	2400	200	400	339.29	235.62	21.02	20	2.77	210	360	FRP	240	0.2	200	1	Bonding
S-hf21	2400	200	400	339.29	235.62	21.02	20	2.77	210	360	FRP	320	0.2	200	1	Bonding
S-hf22	2400	200	400	339.29	235.62	21.02	20	2.77	210	360	FRP	400	0.2	200	1	Bonding
S-hf23	2400	200	400	339.29	235.62	33.23	50	4.38	210	360	FRP	240	0.2	200	1	Bonding
S-hf24	2400	200	400	339.29	235.62	33.23	50	4.38	210	360	FRP	320	0.2	200	1	Bonding
S-hf25	2400	200	400	339.29	235.62	33.23	50	4.38	210	360	FRP	400	0.2	200	1	Bonding
U-t1	2400	200	400	339.29	235.62	25.74	30	3.39	210	360	FRP	400	0.4	200	1	U-jacketing
U-t2	2400	200	400	339.29	235.62	25.74	30	3.39	210	360	FRP	400	0.5	200	1	U-jacketing
U-t3	2400	200	400	339.29	235.62	33.23	50	4.38	210	360	FRP	320	0.1	200	1	U-jacketing
U-t4	2400	200	400	339.29	235.62	33.23	50	4.38	210	360	FRP	320	0.2	200	1	U-jacketing
U-t5	2400	200	400	339.29	235.62	33.23	50	4.38	210	360	FRP	320	0.3	200	1	U-jacketing
U-E6	2400	200	400	339.29	235.62	25.74	30	3.39	210	360	FRP	400	0.2	165	1	U-jacketing
U-E7	2400	200	400	339.29	235.62	25.74	30	3.39	210	360	FRP	400	0.2	244	1	U-jacketing
U-E8	2400	200	400	339.29	235.62	25.74	30	3.39	210	360	FRP	400	0.1	165	1	U-jacketing
U-E9	2400	200	400	339.29	235.62	25.74	30	3.39	210	360	FRP	400	0.1	230	1	U-jacketing
U-E10	2400	200	400	339.29	235.62	25.74	30	3.39	210	360	FRP	400	0.1	244	1	U-jacketing
U-b11	2400	160	400	339.29	235.62	25.74	30	3.39	210	360	FRP	400	0.2	200	1	U-jacketing
U-b12	2400	240	400	339.29	235.62	25.74	30	3.39	210	360	FRP	400	0.2	200	1	U-jacketing
U-b13	2400	300	400	339.29	235.62	25.74	30	3.39	210	360	FRP	400	0.2	200	1	U-jacketing
U-b14	2400	360	400	339.29	235.62	25.74	30	3.39	210	360	FRP	400	0.2	200	1	U-jacketing
U-fc15	2400	200	400	339.29	235.62	21.02	20	2.77	210	360	FRP	400	0.2	200	1	U-jacketing
U-fc16	2400	200	400	339.29	235.62	23.50	25	3.10	210	360	FRP	400	0.2	200	1	U-jacketing
U-fc17	2400	200	400	339.29	235.62	29.73	40	3.92	210	360	FRP	400	0.2	200	1	U-jacketing
U-fc18	2400	200	400	339.29	235.62	23.50	25	3.10	210	360	FRP	400	0.1	200	1	U-jacketing
U-fc19	2400	200	400	339.29	235.62	29.73	40	3.92	210	360	FRP	400	0.1	200	1	U-jacketing
U-hf20	2400	200	400	339.29	235.62	21.02	20	2.77	210	360	FRP	240	0.2	200	1	U-jacketing
U-hf21	2400	200	400	339.29	235.62	21.02	20	2.77	210	360	FRP	320	0.2	200	1	U-jacketing
U-hf22	2400	200	400	339.29	235.62	21.02	20	2.77	210	360	FRP	400	0.2	200	1	U-jacketing
U-hf23	2400	200	400	339.29	235.62	33.23	50	4.38	210	360	FRP	240	0.2	200	1	U-jacketing
U-hf24	2400	200	400	339.29	235.62	33.23	50	4.38	210	360	FRP	320	0.2	200	1	U-jacketing
U-hf25	2400	200	400	339.29	235.62	33.23	50	4.38	210	360	FRP	400	0.2	200	1	U-jacketing
W-C1	2400	200	400	339.29	235.62	25.74	30	3.39	210	360	CFRP	400	0.1	150	1	Wrapped
W-C2	2400	200	400	339.29	235.62	25.74	30	3.39	210	360	CFRP	400	0.1	165	1	Wrapped
W-C3	2400	200	400	339.29	235.62	25.74	30	3.39	210	360	CFRP	400	0.1	230	1	Wrapped
W-A4	2400	200	400	339.29	235.62	25.74	30	3.39	210	360	CFRP	400	0.2	73.0	1	Wrapped
W-A5	2400	200	400	339.29	235.62	25.74	30	3.39	210	360	AFRP	400	0.2	75.9	1	Wrapped
W-A6	2400	200	400	339.29	235.62	25.74	30	3.39	210	360	AFRP	400	0.2	87.0	1	Wrapped
W-A7	2400	200	400	339.29	235.62	25.74	30	3.39	210	360	AFRP	400	0.2	91.0	1	Wrapped
W-A8	2400	200	400	339.29	235.62	25.74	30	3.39	210	360	AFRP	400	0.2	120	1	Wrapped
Kim [117]																
A1	2250	114	150	51.00	0	31.5	56.4	4.5	----	----	AFRP	----	----	60	----	----
A2	2250	114	150	51.00	0	31.5	56.4	4.5	----	----	AFRP	----	----	60	----	----
A3	2250	114	150	51.00	0	31.5	56.4	4.5	----	----	AFRP	----	----	60	----	----
A4	2250	114	150	51.00	0	31.5	56.4	4.5	----	----	AFRP	----	----	60	----	----

B1	2000	150	260	57.60	200	25.4	40.3	3.8	----	----	AFRP	----	----	68	----	----
B2	2000	150	260	57.60	200	25.4	40.3	3.8	----	----	AFRP	----	----	68	----	----
B3	2000	150	260	57.60	200	25.4	40.3	3.8	----	----	AFRP	----	----	68	----	----
B4	2000	150	260	57.60	200	25.4	40.3	3.8	----	----	AFRP	----	----	68	----	----
C1	2400	100	200	33.00	0	39.1	68.5	5.0	----	----	AFRP	----	----	68	----	----
C2	2400	100	200	33.00	0	39.1	68.5	5.0	----	----	AFRP	----	----	68	----	----
C3	2400	100	200	33.00	0	39.1	68.5	5.0	----	----	AFRP	----	----	68	----	----
C4	2400	100	200	33.00	0	39.1	68.5	5.0	----	----	AFRP	----	----	68	----	----
Abbas [118]																
A1	3000	200	300	339	226	27	25	3.5	210	460	----	----	----	----	----	----
A2	3000	200	300	339	226	27	25	3.5	210	460	CFRP	50	1	150	1	Bonding
A3	3000	200	300	339	226	27	25	3.5	210	460	SP	200	30	210	1	Bonding
B1	4000	200	300	226	339	27	25	3.5	210	460	----	----	----	----	----	----
B2	4000	200	300	226	339	27	25	3.5	210	460	CFRP	50	1	150	2	Bonding
B3	4000	200	300	226	339	27	25	3.5	210	460	SP	200	30	210	2	Bonding
Wen-sheng and kai [119]																
L1	2800	180	260	226	226	29.12	25	3.5	210	310	----	----	----	----	----	----
L2	2800	180	260	226	226	29.12	25	3.5	210	310	CFRP	180	0.111	220.5	1	Bonding
L3	2800	180	260	226	226	29.12	25	3.5	210	310	CFRP	180	0.111	220.5	2	Bonding
L4	2800	180	260	226	226	29.12	25	3.5	210	310	CFRP	180	0.111	220.5	3	Bonding
Saifullah, Hossain, Uddin, Khan and Amin [120]																
A	4875	375	500	254.47	0	24.85	27.58	3.27	200	414	SP	375	31.75	200	3	Bonding
B	4875	375	500	254.47	0	24.85	27.58	3.27	200	414	SP	375	31.75	200	3	Bonding
C	4875	375	500	254.47	0	24.85	27.58	3.27	200	414	SP	375	31.75	200	3	Bonding
D	4875	375	500	254.47	0	24.85	27.58	3.27	200	414	SP	375	31.75	200	3	Bonding
E	4875	375	500	254.47	0	24.85	27.58	3.27	200	414	SP	375	31.75	200	3	Bonding
Zhou, Qi and Shi [121]																
ZL3	3200	200	300	226.19	100.53	33.1	32.12	3.15	205	370	CFRP	100	0.11	21.3	1	Bonding
ZL5	3200	200	300	226.19	100.53	33.1	32.12	3.15	205	370	CFRP	100	0.11	21.3	2	Bonding
Hawileh [122]																
C-B	2800	150	280	226.19	56.55	30.3	37.4	3.0	210	600	----	----	----	----	----	None
SC6-1	2800	150	280	226.19	56.55	28.4	37.5	3.4	210	600	CFRP	6	6	146	2	Bonding
SC6-2	2800	150	280	226.19	56.55	27.9	36.5	3.2	210	600	CFRP	6	6	146	2	Bonding
SC6-3	2800	150	280	226.19	56.55	28.1	36.7	3.2	210	600	CFRP	6	6	146	2	Bonding
SC6-4	2800	150	280	226.19	56.55	41.3	66.5	5.4	210	600	CFRP	6	6	146	2	Bonding
SC6-5	2800	150	280	226.19	56.55	27.5	38.1	3.3	210	600	CFRP	6	6	146	2	Bonding
SC12-1	2800	150	280	226.19	56.55	29.5	35.1	3.4	210	600	CFRP	12	12	146	1	Bonding
SC12-2	2800	150	280	226.19	56.55	40.5	67.2	5.6	210	600	CFRP	12	12	146	1	Bonding
Godat, Neale and Labossière [123]																
B-1	2600	150	200	226.19	113.09	26.14	34	3.49	205	391	----	----	----	----	----	None
B-8	2600	150	200	226.19	113.09	26.14	34	3.49	205	391	FRP	150	0.167	22.67	1	U-wrap
TRD1	2700	150	300	226.19	113.09	25.39	31.4	3.36	200	548	----	----	----	----	----	None
TRD3	2700	150	300	226.19	113.09	25.39	31.4	3.36	200	548	FRP	150	0.165	23.67	1	Side bond
TRD4	2700	150	300	226.19	113.09	25.39	31.4	3.36	200	548	FRP	150	0.165	23.67	2	Side bond

TRD2	2700	150	300	226.19	113.09	25.39	31.4	3.36	200	548	FRP	150	0.165	23.67	3	Side bond
BT1	3050	150	405	226.19	113.09	26.42	35	3.55	210	470	----	----	----	----	----	None
BT2	3050	150	405	226.19	113.09	26.42	35	3.55	210	470	FRP	150	0.165	22.83	1	U-wrap
BT3	3050	150	405	226.19	113.09	26.42	35	3.55	210	470	FRP	150	0.165	22.83	2	U-wrap
BT4	3050	150	405	226.19	113.09	26.42	35	3.55	210	470	FRP	150	0.165	22.83	1	U-wrap
BT5	3050	150	405	226.19	113.09	26.42	35	3.55	210	470	FRP	150	0.165	22.83	1	Side bond
BT6	3050	150	405	226.19	113.09	26.42	35	3.55	210	470	FRP	150	0.165	22.83	1	U-wrap
US	1300	150	250	226.19	113.09	26.42	35	3.55	200	400	----	----	----	----	----	None
RS90	1300	150	250	226.19	113.09	26.42	35	3.55	200	400	FRP	150	1.00	17.14	1	Side bond
RS135	1300	150	250	226.19	113.09	26.42	35	3.55	200	400	FRP	150	1.00	17.14	1	Side bond
Ferreira, Bairan and Mari [124]																
DW	2070	130	190	402.12	56.55	28	29	2.6	201	448	FRP	----	----	----	----	----
RW2	2070	130	190	402.12	56.55	29	32	3.3	201	448	FRP	----	----	----	----	----
WB1	2070	130	190	402.12	56.55	29	32	3.3	201	448	FRP	----	----	----	----	----
WB1R	2070	130	190	402.12	56.55	23	36	4.5	201	448	FRP	----	----	----	----	----
Gao, Kim and Leung [125]																
Ga1	2000	150	200	157.1	100.5	31	43.1	3.5	200	531	CFRP	75	0.44	235	1	Bonding
Gb1	2000	150	200	157.1	100.5	25	30	2.9	200	531	CFRP	150	0.44	235	1	Bonding
Gb2	2000	150	200	157.1	100.5	25	30	2.9	200	531	CFRP	150	0.66	235	1	Bonding
Maalej and Bian [126]																
MB3	1500	115	150	235.6	157.1	26	30.3	2.9	183.6	534	CFRP	115	0.222	230	2	Bonding
MB4	1500	115	150	235.6	157.1	26	30.3	2.9	183.6	534	CFRP	115	0.333	230	3	Bonding
MB5	1500	115	150	235.6	157.1	26	30.3	2.9	183.6	534	CFRP	115	0.444	230	4	Bonding
Rahimi and Hutchinson [127]																
RHB5	2300	200	150	157.1	100.5	34.2	52.3	3.83	210	575	CFRP	150	1.2	127	1	Bonding
RHB6	2300	200	150	157.1	100.5	34.2	52.3	3.83	210	575	CFRP	150	1.2	127	1	Bonding
Fanning and Kelly [128]																
FKF5	3000	155	240	339.3	226.2	39.2	80	5	204	532	CFRP	120	1.2	155	1	Bonding
FKF6	3000	155	240	339.3	226.2	39.2	80	5	204	532	CFRP	120	1.2	155	1	Bonding
FKF7	3000	155	240	339.3	226.2	39.2	80	5	204	532	CFRP	120	1.2	155	1	Bonding
FKF10	3000	155	240	339.3	226.2	39.2	80	5	204	532	CFRP	120	1.2	155	1	Bonding
Quantrill, Hollaway and Thorne [129]																
B2	1000	100	100	84.8	56.5	32	45.1	3.56	215	350	FRP	80	1.2	49	----	Bonding
B4	1000	100	100	84.8	56.5	32	45.1	3.56	215	350	FRP	60	1.6	49	----	Bonding
Quantrill, Hollaway and Thorne [130]																
A1c	1000	100	100	84.8	56.5	36.5	59.5	4.1	210	350	FRP	80	1.2	49	----	Bonding
A2b	1000	100	100	84.8	56.5	28.3	35.7	3.2	210	350	FRP	80	1.2	49	----	Bonding
A2c	1000	100	100	84.8	56.5	28.3	35.7	3.2	210	350	FRP	80	1.2	49	----	Bonding
David, Djelal, Ragneau and Bodin [131]																
P2	2800	150	300	307.9	0	30	40	3.4	200	500	CFRP	100	1.2	150	----	Bonding
P3	2800	150	300	307.9	0	30	40	3.4	200	500	CFRP	100	1.2	150	----	Bonding
P4	2800	150	300	307.9	0	30	40	3.4	200	500	CFRP	100	2.4	150	----	Bonding
P5	2800	150	300	307.9	0	30	40	3.4	200	500	CFRP	100	2.4	150	----	Bonding
Garden, Hollaway and Thorne [132]																

1Au	1000	100	100	84.8	56.5	33.5	50.2	3.8	215	350	CFRP	90	0.5	111	----	Bonding
1Bu	1000	100	100	84.8	56.5	33.5	50.2	3.8	215	350	CFRP	65	0.7	111	----	Bonding
1Cu	1000	100	100	84.8	56.5	33.5	50.2	3.8	215	350	CFRP	45	1.0	111	----	Bonding
2Au	1000	100	100	84.8	56.5	33.5	50.2	3.8	215	350	CFRP	90	0.5	111	----	Bonding
2Bu	1000	100	100	84.8	56.5	33.5	50.2	3.8	215	350	CFRP	65	0.7	111	----	Bonding
2Cu	1000	100	100	84.8	56.5	33.5	50.2	3.8	215	350	CFRP	45	1.0	111	----	Bonding
3Au	1000	100	100	84.8	56.5	33.5	50.2	3.8	215	350	CFRP	90	0.5	111	----	Bonding
3Bu	1000	100	100	84.8	56.5	33.5	50.2	3.8	215	350	CFRP	65	0.7	111	----	Bonding
3Cu	1000	100	100	84.8	56.5	33.5	50.2	3.8	215	350	CFRP	45	1.0	111	----	Bonding
Saadatmanesh and Ehsani [133]																
B	4880	205	455	981.7	265.5	28	35	3.14	200	456	CFRP	152	6	37.2	----	Bonding
C	4880	205	455	265.5	265.5	28	35	3.14	200	456	CFRP	152	6	37.2	----	Bonding
Nguyen, Chan and Cheong [134]																
A950	1500	120	150	235.6	56.5	25	27.3	2.8	200	384	CFRP	80	1.2	181	----	Bonding
A1100	1500	120	150	235.6	56.5	25	27.3	2.8	200	384	CFRP	80	1.2	181	----	Bonding
A1150	1500	120	150	235.6	56.5	25	27.3	2.8	200	384	CFRP	80	1.2	181	----	Bonding
NB2	1500	120	150	628.3	56.5	29.1	37.9	3.23	200	384	CFRP	80	1.2	181	----	Bonding
Gao, Kim and Leung [135]																
1T6LN	2000	150	200	157.1	100.5	32.5	47.8	3.7	200	531	CFRP	150	0.66	235	----	Bonding
2T6LN	2000	150	200	157.1	100.5	37.1	62.1	4.2	200	531	CFRP	150	0.66	235	----	Bonding
2T6La1	2000	150	200	157.1	100.5	37.1	62.1	4.2	200	531	CFRP	150	0.66	235	----	Bonding
2T4LN	2000	150	200	157.1	100.5	37.1	62.1	4.2	200	531	CFRP	150	0.44	235	----	Bonding
2T4La1	2000	150	200	157.1	100.5	37.1	62.1	4.2	200	531	CFRP	150	0.44	235	----	Bonding
Ahmed and Van [136]																
DF2	1500	125	225	150.8	56.5	30	46	3.6	185	568	CFRP	75	0.334	240	----	Bonding
DF3	1500	125	225	150.8	56.5	30	46	3.6	185	568	CFRP	75	0.501	240	----	Bonding
DF4	1500	125	225	150.8	56.5	30	46	3.6	185	568	CFRP	75	0.668	240	----	Bonding
Hung and Li [137]																
AB	3200	102	178	----	78.5	----	----	----	200	414	CFRP	38	0.038	117	----	Bonding

Table 2: Comparison between experimental results and numerical simulation of load-carrying capacity and deflection response of reinforced concrete beams retrofitted with FRP

Test	P_{EXP} (kN)	P_{FE} (kN)	P_{FE}/P_{EXP}	δ_{EXP} (mm)	δ_{FE} (mm)	δ_{FE}/δ_{EXP}	Failure Mode
[112]							
A	36.40	34.57	0.95	14.61	19.49	1.33	Flexure
B	54.48	56.57	1.04	9.98	10.31	1.03	Flexure
C	----	62.50	----	----	19.43	----	Flexure
D	----	68.89	----	----	19.73	----	Flexure
[113]							
A	225	227.1	1.01	68	75	1.10	Flexure
B	397	----	----	----	----	----	Flexure
C	385	----	----	----	----	----	Flexure
D	377	----	----	----	----	----	Flexure
E	399	----	----	----	----	----	Flexure
[114]							
CB1	41.25	41.75	1.01	21.3	21.6	1.01	Flexure
FRP1	49.50	49.00	0.99	22.1	22.4	1.01	Debonding
CB2	69.00	68.00	0.99	8.40	8.90	1.06	Flexure
FRP2	125.0	120.0	0.96	85.91	87.85	1.02	Debonding
[115]							
A1	476	454	0.95	23.13	29.12	1.26	Flexure
B1	689	623	0.90	30.00	22.50	0.75	FRP Rupture
C1	689	525	0.76	34.75	37.75	1.09	FRP Rupture
D1	645	930	1.44	25.00	62.75	2.51	*N/A
[116]							
S-t1	----	188.8	----	----	----	----	Debonding
S-t2	----	198.8	----	----	----	----	Debonding
S-t3	----	184.0	----	----	----	----	Tensile rupture
S-t4	----	196.0	----	----	----	----	Tensile rupture
S-t5	----	204.4	----	----	----	----	Tensile rupture
S-E6	----	170.1	----	----	----	----	Debonding
S-E7	----	179.8	----	----	----	----	Debonding
S-E8	----	159.8	----	----	----	----	Tensile rupture
S-E9	----	166.6	----	----	----	----	Tensile rupture
S-E10	----	169.8	----	----	----	----	Tensile rupture
S-b11	----	203.5	----	----	----	----	Debonding
S-b12	----	228.3	----	----	----	----	Tensile rupture
S-b13	----	245.6	----	----	----	----	Tensile rupture
S-b14	----	265.4	----	----	----	----	Tensile rupture
S-fc15	----	153.4	----	----	----	----	Debonding
S-fc16	----	167.4	----	----	----	----	Debonding
S-fc17	----	191.5	----	----	----	----	Debonding
S-fc18	----	151.7	----	----	----	----	Tensile rupture
S-fc19	----	179.8	----	----	----	----	Tensile rupture
S-hf20	----	157.3	----	----	----	----	Debonding
S-hf21	----	167.6	----	----	----	----	Debonding
S-hf22	----	184.4	----	----	----	----	Debonding
S-hf23	----	215.4	----	----	----	----	Tensile rupture
S-hf24	----	236.9	----	----	----	----	Tensile rupture
S-hf25	----	260.9	----	----	----	----	Tensile rupture
U-t1	----	256.8	----	----	----	----	Debonding
U-t2	----	270.1	----	----	----	----	Debonding
U-t3	----	233.1	----	----	----	----	Tensile rupture
U-t4	----	256.7	----	----	----	----	Tensile rupture
U-t5	----	273.1	----	----	----	----	Tensile rupture
U-E6	----	216.8	----	----	----	----	Debonding
U-E7	----	235.8	----	----	----	----	Debonding
U-E8	----	203.8	----	----	----	----	Tensile rupture

Journal of Advanced Research in Applied Mechanics
ISSN (online): 2289-7895 | Vol. 22, No. 1. Pages 13-48, 2016

U-E9	----	216.8	----	----	----	----	Tensile rupture
U-E10	----	225.3	----	----	----	----	Tensile rupture
U-b11	----	234.5	----	----	----	----	Debonding
U-b12	----	279.1	----	----	----	----	Tensile rupture
U-b13	----	311.0	----	----	----	----	Tensile rupture
U-b14	----	343.9	----	----	----	----	Tensile rupture
U-fc15	----	193.8	----	----	----	----	Debonding
U-fc16	----	212.4	----	----	----	----	Debonding
U-fc17	----	254.5	----	----	----	----	Debonding
U-fc18	----	187.4	----	----	----	----	Tensile rupture
U-fc19	----	234.5	----	----	----	----	Tensile rupture
U-hf20	----	178.3	----	----	----	----	Debonding
U-hf21	----	199.4	----	----	----	----	Debonding
U-hf22	----	221.9	----	----	----	----	Debonding
U-hf23	----	256.4	----	----	----	----	Tensile rupture
U-hf24	----	292.9	----	----	----	----	Tensile rupture
U-hf25	----	335.9	----	----	----	----	Tensile rupture
W-C1	----	238.0	----	----	----	----	Tensile rupture
W-C2	----	244.8	----	----	----	----	Tensile rupture
W-C3	----	266.8	----	----	----	----	Tensile rupture
W-A4	----	195.2	----	----	----	----	Tensile rupture
W-A5	----	197.2	----	----	----	----	Tensile rupture
W-A6	----	201.1	----	----	----	----	Tensile rupture
W-A7	----	203.8	----	----	----	----	Tensile rupture
W-A8	----	213.9	----	----	----	----	Tensile rupture
[117]							
A1	16.6	17.3	1.04	25.8	31.4	1.22	Rupture
A2	17.5	17.3	0.99	39.2	44.7	1.14	Rupture
A3	17.6	17.5	0.99	61.5	70.3	1.14	Rupture
A4	17.7	17.3	0.98	88.6	97.8	1.10	Rupture
B1	87.0	88.9	1.02	20.1	21.3	1.06	Rupture
B2	89.5	91.5	1.02	19.4	33.5	1.73	Rupture
B3	89.0	79.2	0.89	30.9	47.8	1.55	Crush
B4	69.4	67.5	0.97	56.4	61.2	1.09	Crush
C1	7.80	7.40	0.95	37.5	44.3	1.18	Rupture
C2	7.40	7.50	1.01	53.6	60.0	1.12	Rupture
C3	7.20	7.50	1.04	74.8	85.4	1.14	Rupture
C4	7.10	7.70	1.08	87.8	105.1	1.19	Rupture
[118]							
A1	80.0	85.2	1.07	10	12	1.20	Crush
A2	110	125	1.14	25	22	0.88	Debonding
A3	140	140.4	1.00	41	33	0.80	Debonding
B1	----	160	----	----	56	----	Crush
B2	----	235	----	----	25	----	Debonding
B3	----	241	----	----	42	----	Debonding
[119]							
L1	41.0	50	1.22	34	37	1.09	Crush
L2	51.0	48	0.94	28	29	1.04	Debonding
L3	55.0	53	0.96	24	31	1.29	Debonding
L4	60.5	60	0.99	20	21	1.05	Debonding
[120]							
A	----	274.08	----	----	58.67	----	Flexure
B	----	275.88	----	----	102.5	----	Flexure
C	----	275.13	----	----	86.07	----	Flexure
D	----	275.26	----	----	93.67	----	Flexure
E	----	275.63	----	----	87.90	----	Flexure
[121]							
ZL3	92	98.4	1.07	46	37	0.80	Rupture
ZL5	110	114.6	1.04	29	26	0.89	Rupture
[122]							
C-B	29.5	29.04	0.98	60.10	63.0	1.05	Flexure

Journal of Advanced Research in Applied Mechanics
ISSN (online): 2289-7895 | Vol. 22, No. 1. Pages 13-48, 2016

SC6-1	58.5	58.98	1.00	56.72	60.0	1.06	Rod pull out
SC6-2	53.5	53.21	0.99	46.50	50.0	1.08	Rod pull out
SC6-3	44.0	43.64	0.99	27.05	28.0	1.04	Cover separation
SC6-4	65.4	64.50	0.99	40.70	40.0	0.98	Flexure
SC6-5	73.2	72.90	0.99	43.69	46.0	1.05	Rod pull out
SC12-1	59.2	59.05	0.99	51.02	54.0	1.06	Rod pull out
SC12-2	43.9	43.50	0.99	32.56	33.5	1.03	Debonding
[123]							
B-1	40	41	1.02	6.20	6.30	1.02	Diagonal shear
B-8	86	90	1.05	16.0	15.4	0.96	Debonding
TRD1	322	323	1.00	9.80	9.60	0.98	Diagonal shear
TRD3	323	336	1.04	14.5	13.1	0.90	Debonding
TRD4	400	399	0.99	14.0	13.3	0.95	Debonding
TRD2	422	414	0.99	13.0	12.5	0.96	Debonding
BT1	178	184	1.03	7.10	6.50	0.92	Diagonal shear
BT2	309	313	1.01	7.00	7.40	1.06	Debonding
BT3	310	313	1.01	7.00	6.90	0.99	Debonding
BT4	324	325	1.00	8.50	8.40	0.99	Debonding
BT5	243	247	1.02	6.20	6.00	0.97	Debonding
BT6	442	453	1.03	22.0	21.9	0.99	Crush
US	114	119	1.04	3.00	2.90	0.97	Diagonal shear
RS90	184	197	1.07	4.00	4.00	1.00	Debonding
RS135	194	202	1.04	6.00	5.90	0.98	Debonding
[124]							
DW	38	39	1.03	10	9	0.90	Diagonal Shear
RW2	88	91	1.03	11	13	1.18	Diagonal Shear
WB1	27	28	1.04	6	5	0.83	Diagonal Shear
WB1R	91	90	0.99	10	12	1.20	Diagonal Shear
[125]							
Ga1	92	114.8	1.25	11.6	----	----	Cover separation
Gb1	76	83.2	1.09	9.8	----	----	Cover separation
Gb2	75	83.3	1.11	10.8	----	----	Cover separation
[126]							
MB3	86	73.5	0.86	17.0	12	0.71	Cover separation
MB4	82	70.4	0.86	13.2	7	0.53	Cover separation
MB5	79	70.9	0.90	10.0	6	0.60	Cover separation
[127]							
RHB5	69.7	62.0	0.89	25	----	----	Cover separation
RHB6	69.6	62.0	0.89	31	----	----	Cover separation
[128]							
FKF5	100	100.9	1.01	22	----	----	Cover separation
FKF6	103	100.9	0.98	21	----	----	Cover separation
FKF7	97.5	99.9	1.02	14	----	----	Cover separation
FKF10	82.0	98.9	1.21	13	----	----	Cover separation
[129]							
B2	34	34.5	1.02	----	----	----	Cover separation
B4	35	37.6	1.07	----	----	----	Cover separation
[130]							
A1c	44.0	32.6	0.74	----	----	----	Cover separation
A2b	36.7	35.5	0.97	----	----	----	Cover separation
A2c	37.3	35.5	0.95	----	----	----	Cover separation
[131]							
P2	136.0	109.4	0.80	----	----	----	Cover separation
P3	142.2	109.4	0.77	----	----	----	Cover separation
P4	156.0	105.4	0.68	----	----	----	Cover separation
P5	159.0	105.4	0.66	----	----	----	Cover separation
[132]							
1Au	39.6	37.8	0.95	----	----	----	Cover separation
1Bu	36.5	38.1	1.04	----	----	----	Cover separation
1Cu	31.9	37.8	1.19	----	----	----	Cover separation
2Au	38.5	37.8	0.98	----	----	----	Cover separation

Penerbit Akademia Baru

Journal of Advanced Research in Applied Mechanics
ISSN (online): 2289-7895 | Vol. 22, No. 1. Pages 13-48, 2016

2Bu	34.0	38.1	1.12	----	----	----	Cover separation
2Cu	35.5	37.8	1.07	----	----	----	Cover separation
3Au	39.0	37.8	0.97	----	----	----	Cover separation
3Bu	34.5	38.1	1.10	----	----	----	Cover separation
3Cu	30.7	37.8	1.23	----	----	----	Cover separation
[133]							
B	250	238.4	0.95	----	----	----	Cover separation
C	190	117.6	0.62	----	----	----	Cover separation
[134]							
A950	56.2	43.6	0.78	----	----	----	Cover separation
A1100	57.3	53.2	0.93	----	----	----	Cover separation
A1150	58.9	59.8	1.02	----	----	----	Cover separation
NB2	130.1	103.1	0.79	----	----	----	Cover separation
[135]							
1T6LN	116.2	162.4	1.40	----	----	----	Cover separation
2T6LN	135.9	153.5	1.13	----	----	----	Cover separation
2T6La1	139.6	153.5	1.10	----	----	----	Cover separation
2T4LN	133.3	92.9	0.70	----	----	----	Cover separation
2T4La1	137.7	92.9	0.67	----	----	----	Cover separation
[136]							
DF2	120.6	82.0	0.68	----	----	----	Cover separation
DF3	120.0	96.0	0.80	----	----	----	Cover separation
DF4	125.6	109.5	0.87	----	----	----	Cover separation
[137]							
AB	63	65	1.03	8	8.5	1.06	Flexure

Load – carrying capacity (P_{FE}/P_{EXP}) for retrofitted reinforced concrete beams (FRP beams)					
All (91)	Mean = 0.99	St. Dev. = 0.14	COV = 0.14	Min. = 0.62	Max. = 1.44
Flexure (3)	Mean = 1.00	St. Dev. = 0.03	COV = 0.03	Min. = 0.95	Max. = 1.04
Debonding (18)	Mean = 1.01	St. Dev. = 0.04	COV = 0.04	Min. = 0.94	Max. = 1.14
FRP rupture (5)	Mean = 1.03	St. Dev. = 0.23	COV = 0.22	Min. = 0.76	Max. = 1.44
Tensile rupture (10)	Mean = 1.01	St. Dev. = 0.04	COV = 0.04	Min. = 0.95	Max. = 1.08
Crush (2)	Mean = 1.04	St. Dev. = 1.12	COV = 0.12	Min. = 0.89	Max. = 1.22
Rod pull out (4)	Mean = 0.99	St. Dev. = 0.01	COV = 0.01	Min. = 0.99	Max. = 1.00
Cover separation (45)	Mean = 0.95	St. Dev. = 0.18	COV = 0.19	Min. = 0.66	Max. = 1.25
Diagonal shear (4)	Mean = 1.02	St. Dev. = 0.02	COV = 0.02	Min. = 0.99	Max. = 1.04
Deflection (δ_{FE}/δ_{EXP}) for retrofitted reinforced concrete beams (FRP beams)					
All (50)	Mean = 1.06	St. Dev. = 0.26	COV = 0.25	Min. = 0.53	Max. = 2.51
Flexure (3)	Mean = 1.09	St. Dev. = 0.12	COV = 0.11	Min. = 0.98	Max. = 1.33
Debonding (18)	Mean = 0.99	St. Dev. = 0.09	COV = 0.09	Min. = 0.80	Max. = 1.29
FRP rupture (5)	Mean = 1.22	St. Dev. = 0.66	COV = 0.54	Min. = 0.75	Max. = 2.51
Tensile rupture (10)	Mean = 1.20	St. Dev. = 0.19	COV = 0.16	Min. = 1.06	Max. = 1.73
Crush (2)	Mean = 1.18	St. Dev. = 0.22	COV = 0.18	Min. = 0.99	Max. = 1.55
Rod pull out (4)	Mean = 1.06	St. Dev. = 0.01	COV = 0.01	Min. = 1.05	Max. = 1.08
Cover separation (4)	Mean = 0.72	St. Dev. = 0.23	COV = 0.31	Min. = 0.53	Max. = 1.04
Diagonal shear (4)	Mean = 1.00	St. Dev. = 0.13	COV = 0.13	Min. = 0.83	Max. = 1.20
Load – carrying capacity (P_{FE}/P_{EXP}) for reference reinforced concrete beams (without FRP)					
All (13)	Mean = 1.02	St. Dev. = 0.07	COV = 0.07	Min. = 0.95	Max. = 1.22
Flexure (6)	Mean = 0.98	St. Dev. = 0.03	COV = 0.03	Min. = 0.95	Max. = 1.01
Crush (3)	Mean = 1.11	St. Dev. = 0.10	COV = 0.09	Min. = 1.03	Max. = 1.22
Diagonal shear (4)	Mean = 1.02	St. Dev. = 0.02	COV = 0.02	Min. = 1.00	Max. = 1.04
Deflection (δ_{FE}/δ_{EXP}) for reference reinforced concrete beams (without FRP)					
All (13)	Mean = 1.08	St. Dev. = 0.12	COV = 0.11	Min. = 0.92	Max. = 1.33
Flexure (6)	Mean = 1.14	St. Dev. = 0.13	COV = 0.11	Min. = 1.01	Max. = 1.33
Crush (3)	Mean = 1.09	St. Dev. = 0.11	COV = 0.09	Min. = 0.99	Max. = 1.20
Diagonal shear (4)	Mean = 0.97	St. Dev. = 0.04	COV = 0.04	Min. = 0.92	Max. = 1.02

* The specimen did not fail.

Journal of Advanced Research in Applied Mechanics
ISSN (online): 2289-7895 | Vol. 22, No. 1. Pages 13-48, 2016

4.0 CONCLUSIONS AND RECOMMENDATIONS FOR FUTURE RESEARCH

External bonding of fiber reinforced plastic FRP (strips, plates or rods) can significantly improve the ultimate strength and ductility of strengthened reinforced concrete beams. The ultimate load - carrying capacity has been studied for both reference and FRP reinforced concrete beams as well as deflection responses of the specimens. Experimental measurements and numerical simulations are compared based on numerous tests available in the collected data which adopted in the current study. Furthermore, the finite element results which obtained by the researchers have been achieved using very fine meshes built employing the ANSYS software elements package.

Based on the gathered data, the effects of individual parameters for the flexure, debonding, FRP rupture, concrete crushing, rod pull out, diagonal shear, cover separation and tensile rupture failure cases were carried out, and the following conclusions observed:

- The research showed that after the rehabilitation of reinforced concrete beam strengthened with different type of fibers, the deflection of its mid-span reduced, the bearing capacity of reinforced concrete beam was increased with the numbers of fiber sheets increased. The deflection of FRP beams significantly decreased compared to the reference reinforced concrete beams while the ultimate loads were increased.
- There were several parameters that effect on the retrofitted beams by increasing beams strength and stiffness of FRP strengthened beam. These parameters involved beam width, FRP thickness, concrete strength, height of FRP sheet and FRP modulus of elasticity.
- It was demonstrated that the experimental test and analytical modeling were quite similar in trend of the behavior of load, displacement and stress levels for most of the models studied in this research. In addition, the specific and accurate information has been provided on the status of the failure experienced by the real structural system.

More information on FRP modeling would help to establish a greater degree of accuracy on this matter. If the debate is to be moved forward, a better understanding of using FRP composites in structural member needs to be developed. It is recommended that further research be undertaken of utilizing nonlinear analysis modeling in the following areas:

- The material type of contact layer between FRP material and RC section.
- Fire resistance.
- Thermal resistance.
- The type of FRP used in the construction of structures in seismic zones.
- Statistical study on the cost, construction speed and reduce environmental impacts of structures.

Journal of Advanced Research in Applied Mechanics
ISSN (online): 2289-7895 | Vol. 22, No. 1. Pages 13-48, 2016

ACKNOWLEDGEMENTS

The researchers gratefully acknowledge the technical support provided by Faculty of Civil Engineering at University of Gaziantep.

REFERENCES

[1] Nawy, E.G., Fundamentals of high strength high performance concrete. 1996: Addison-Wesley Longman.

[2] Mohammadi, Y., S.P. Singh, and S.K. Kaushik, Properties of steel fibrous concrete containing mixed fibres in fresh and hardened state. Construction and Building Materials, 2008. 22(5): p. 956-965.

[3] Hadi, M., Reinforcing concrete columns with steel fibres. Asian Journal of Civil Engineering (Building and Housing), 2009. 10(1): p. 79-95.

[4] Iskhakov, I. and Y. Ribakov, A design method for two-layer beams consisting of normal and fibered high strength concrete. Materials & Design, 2007. 28(5): p. 1672-1677.

[5] Gan, M., Cement and concrete. 1997: CRC Press.

[6] Heinzle, G., B. Freytag, and J. Linder, Rissbildung von biegebeanspruchten Bauteilen aus Ultrahochfestem Faserbeton. Beton-und Stahlbetonbau, 2009. 104(9): p. 570-580.

[7] Wang, Z.L., J. Wu, and J.G. Wang, Experimental and numerical analysis on effect of fibre aspect ratio on mechanical properties of SRFC. Construction and Building Materials, 2010. 24(4): p. 559-565.

[8] Singh, B., P. Kumar, and S. Kaushik, High performance composites for the new millennium. Journal of Structural Engineering, 2001. 28(1): p. 17-26.

[9] Ganesan, N. and K. Shivananda, Strength and ductility of latex modified steel fibre reinforced concrete flexural members. Journal of Structural Engineering, 2000. 27(2): p. 111-116.

[10] Holschemacher, K., T. Mueller, and Y. Ribakov, Effect of steel fibres on mechanical properties of high-strength concrete. Materials & Design, 2010. 31(5): p. 2604-2615.

[11] Topcu, I.B. and M. Canbaz, Effect of different fibers on the mechanical properties of concrete containing fly ash. Construction and Building Materials, 2007. 21(7): p. 1486-1491.

[12] Wang, C., Experimental investigation on behavior of steel fiber reinforced concrete, in University of Canterbury. Civil Engineering. 2006, University of Canterbury: New Zealand.

[13] Barnett, S.J., et al., Assessment of fibre orientation in ultra high performance fibre reinforced concrete and its effect on flexural strength. Materials and Structures, 2010. 43(7): p. 1009-1023.

[14] Yang, S.L., et al., Influence of aggregate and curing regime on the mechanical properties of ultra-high performance fibre reinforced concrete (UHPFRC). Construction and Building Materials, 2009. 23(6): p. 2291-2298.

[15] Fan, H.L., et al., Mechanics of advanced fiber reinforced lattice composites. Acta Mechanica Sinica, 2010. 26(6): p. 825-835.

[16] Fan, H.L., F.H. Meng, and W. Yang, Mechanical behaviors and bending effects of carbon fiber reinforced lattice materials. Archive of Applied Mechanics, 2006. 75(10-12): p. 635-647.

[17] Ganesan, N. and T. Sekar, Permeability of steel fibre reinforced high performance concrete composites. Journal of the Institution of Engineers(India), Part CV, Civil Engineering Division, 2005. 86: p. 8-11.

[18] Brühwiler, E. and E. Denarie. Rehabilitation of concrete structures using ultra-high performance fibre reinforced concrete. in Proceedings, The Second International Symposium on Ultra-High Performance Concrete. 2008. Citeseer.

[19] Buchan, P.A. and J.F. Chen, Blast resistance of FRP composites and polymer strengthened concrete and masonry structures - A state-of-the-art review. Composites Part B-Engineering, 2007. 38(5-6): p. 509-522.

[20] Hawileh, R.A., T.A. El-Maaddawy, and M.Z. Naser, Nonlinear finite element modeling of concrete deep beams with openings strengthened with externally-bonded composites. Materials & Design, 2012. 42: p. 378-387.

[21] Maaddawy, T.E., M.E. Sayed, and B. Abdel-Magid, The effects of cross-sectional shape and loading condition on performance of reinforced concrete members confined with Carbon Fiber-Reinforced Polymers. Materials & Design, 2010. 31(5): p. 2330-2341.

[22] Turgay, T., et al., Stress-strain model for concrete confined with CFRP jackets. Materials & Design, 2009. 30(8): p. 3243-3251.

[23] Keller, T., Use of fibre reinforced polymers in bridge construction. 2003.

[24] Bakis, C.E., et al., Fiber-reinforced polymer composites for construction-state-of-the-art review. Journal of Composites for Construction, 2002. 6(2): p. 73-87.

[25] Hawileh, R.A., et al., Behavior of reinforced concrete beams strengthened with externally bonded hybrid fiber reinforced polymer systems. Materials & Design, 2014. 53: p. 972-982.

[26] Sakar, G., et al., Nonlinear behavior of shear deficient RC beams strengthened with near surface mounted glass fiber reinforcement under cyclic loading. Materials & Design, 2014. 61: p. 16-25.

[27] De Lorenzis, L. and J. Teng, Near-surface mounted FRP reinforcement: An emerging technique for strengthening structures. Composites Part B: Engineering, 2007. 38(2): p. 119-143.

[28] Barros, J.A.O., S.J.E. Dias, and J.L.T. Lima, Efficacy of CFRP-based techniques for the flexural and shear strengthening of concrete beams. Cement & Concrete Composites, 2007. 29(3): p. 203-217.

[29] Seracino, R., M.R.R. Saifulnaz, and D.J. OehlerS, Generic debonding resistance of EB and NSM plate-to-concrete joints. Journal of Composites for Construction, 2007. 11(1): p. 62-70.

[30] El-Hacha, R. and S.H. Rizkalla, Near-surface-mounted fiber-reinforced polymer reinforcements for flexural strengthening of concrete structures. Aci Structural Journal, 2004. 101(5): p. 717-726.

[31] Smith, S.T. and J.G. Teng, FRP-strengthened RC beams. I: review of debonding strength models. Engineering Structures, 2002. 24(4): p. 385-395.

[32] Chen, J.F. and J.G. Teng, Shear capacity of FRP-strengthened RC beams: FRP debonding. Construction and Building Materials, 2003. 17(1): p. 27-41.

[33] Yang, Z.J., J.F. Chen, and D. Proverbs, Finite element modelling of concrete cover separation failure in FRP plated RC beams. Construction and Building Materials, 2003. 17(1): p. 3-13.

[34] Ombres, L., Prediction of intermediate crack debonding failure in FRP-strengthened reinforced concrete beams. Composite Structures, 2010. 92(2): p. 322-329.

[35] Chen, J.F. and J.G. Teng, Anchorage strength models for FRP and steel plates bonded to concrete. Journal of Structural Engineering-Asce, 2001. 127(7): p. 784-791.

[36] Nilson, A.H. Nonlinear analysis of reinforced concrete by the finite element method. in ACI Journal Proceedings. 1968. ACI.

[37] Ngo, D. and A. Scordelis. Finite element analysis of reinforced concrete beams. in ACI Journal Proceedings. 1967. ACI.

[38] Doran, B., H.O. Koksal, and T. Turgay, Nonlinear finite element modeling of rectangular/square concrete columns confined with FRP. Materials & Design, 2009. 30(8): p. 3066-3075.

[39] Li, L.J., et al., Interfacial stress analysis of RC beams strengthened with hybrid CFS and GFS. Construction and Building Materials, 2009. 23(6): p. 2394-2401.

[40] Akbarzadeh, H. and A.A. Maghsoudi, Experimental and analytical investigation of reinforced high strength concrete continuous beams strengthened with fiber reinforced polymer. Materials & Design, 2010. 31(3): p. 1130-1147.

[41] Rashid, Y., Ultimate strength analysis of prestressed concrete pressure vessels. Nuclear engineering and design, 1968. 7(4): p. 334-344.

[42] Suidan, M. and W.C. Schnobrich, Finite element analysis of reinforced concrete. Journal of the Structural Division, 1973. 99(10): p. 2109-2122.

Journal of Advanced Research in Applied Mechanics
ISSN (online): 2289-7895 | Vol. 22, No. 1. Pages 13-48, 2016

[43] Yang, Q.S., Q.H. Qin, and D.H. Zheng, Analytical and numerical investigation of interfacial stresses of FRP-concrete hybrid structure. Composite Structures, 2002. 57(1-4): p. 221-226.

[44] Camata, G., E. Spacone, and R. Zarnic, Experimental and nonlinear finite element studies of RC beams strengthened with FRP plates. Composites Part B-Engineering, 2007. 38(2): p. 277-288.

[45] Bangash, M., Concrete and concrete structures: numerical modelling and applications. 1989.

[46] Huyse, L., Y. Hemmaty, and L. Vandewalle. Finite element modeling of fiber reinforced concrete beams. in Proceedings of the ANSYS Conference. 1994.

[47] Padmarajaiah, S.K. and A. Ramaswamy, A finite element assessment of flexural strength of prestressed concrete beams with fiber reinforcement. Cement & Concrete Composites, 2002. 24(2): p. 229-241.

[48] Barros, J.A.O. and A.S. Fortes, Flexural strengthening of concrete beams with CFRP laminates bonded into slits. Cement & Concrete Composites, 2005. 27(4): p. 471-480.

[49] Varma, R., J.A. Barros, and J. Sena-Cruz, Fibrous model for the simulation of the cyclic behaviour of 3D reinforced concrete frames. 2007.

[50] Collins, M., et al., Analytical modelling of reinforced concrete subjected to monotonic and reversed loadings. 1987: University of Toronto, Department of Civil Engineering.

[51] Arduini, M. and A. Nanni, Behavior of precracked RC beams strengthened with carbon FRP sheets. Journal of Composites for Construction, 1997. 1(2): p. 63-70.

[52] Abdul-Ahad, R.B. and O.Q. Aziz, Flexural strength of reinforced concrete T-beams with steel fibers. Cement and Concrete Composites, 1999. 21(4): p. 263-268.

[53] Attari, N., S. Amziane, and M. Chemrouk, Flexural strengthening of concrete beams using CFRP, GFRP and hybrid FRP sheets. Construction and Building Materials, 2012. 37: p. 746-757.

[54] Arduini, M., A. Di Tommaso, and A. Nanni, Brittle failure in FRP plate and sheet bonded beams. ACI Structural Journal, 1997. 94(4).

[55] Bank, L. Mechanically Fastened FRP (MF-FRP) Strips for Strengthening RC Structures–A Viable Alternative. in Proc of 2nd international conference on FRP composites in civil engineering: CICE, Adelaide, Australia. 2004.

[56] Lamanna, A.J., L.C. Bank, and D.W. Scott, Flexural strengthening of reinforced concrete beams using fasteners and fiber-reinforced polymer strips. Aci Structural Journal, 2001. 98(3): p. 368-376.

[57] Ekenel, M., et al., Flexural fatigue behavior of reinforced concrete beams strengthened with FRP fabric and precured laminate systems. Journal of Composites for Construction, 2006. 10(5): p. 433-442.

[58] Martin, J.A. and A.J. Lamanna, Performance of mechanically fastened FRP strengthened concrete beams in flexure. Journal of Composites for Construction, 2008. 12(3): p. 257-265.

[59] Sena-Cruz, J., et al., Numerical simulation of the nonlinear behavior of RC beams strengthened with NSM CFRP strips. 2007.

[60] Bonaldo, E., Composite materials and discrete steel fibres for the strengthening of thin concrete structures. 2008.

[61] An, W., H. Saadatmanesh, and M.R. Ehsani, RC beams strengthened with FRP plates. II: Analysis and parametric study. Journal of Structural Engineering, 1991. 117(11): p. 3434-3455.

[62] Rabinovitch, O. and Y. Frostig, Experiments and analytical comparison of RC beams strengthened with CFRP composites. Composites Part B-Engineering, 2003. 34(8): p. 663-677.

[63] Thomsen, H., et al., Failure mode analyses of reinforced concrete beams strengthened in flexure with externally bonded fiber-reinforced polymers. Journal of Composites for Construction, 2004. 8(2): p. 123-131.

[64] Bank, L.C. and D. Arora, Analysis of RC beams strengthened with mechanically fastened FRP (MF-FRP) strips. Composite Structures, 2007. 79(2): p. 180-191.

[65] Ashour, A.F., S.A. El-Refaie, and S.W. Garrity, Flexural strengthening of RC continuous beams using CFRP laminates. Cement & Concrete Composites, 2004. 26(7): p. 765-775.

[66] El-Mihilmy, M.T. and J.W. Tedesco, Analysis of reinforced concrete beams strengthened with FRP laminates. Journal of Structural Engineering-Asce, 2000. 126(6): p. 684-691.

[67] Rasheed, H.A., H. Charkas, and H. Melhem, Simplified nonlinear analysis of strengthened concrete beams based on a rigorous approach. Journal of Structural Engineering-Asce, 2004. 130(7): p. 1087-1096.

[68] ANSYS, A.U.s.M.R., 5.5, ANSYS. Inc., Canonsburg, Pennsylvania, 1998.

[69] Shah, S.P., S.E. Swartz, and C. Ouyang, Fracture mechanics of concrete. W C iley, New York, W 1995, 1995.

[70] Barbosa, A.F. and G.O. Ribeiro, Analysis of reinforced concrete structures using ANSYS nonlinear concrete model. 1998.

[71] Hughes, G. and D. Speirs, An investigation of the beam impact problem. 1982.

[72] Zhou, M.R., Application of Finite Element Method for Nonlinear Analysis in Reinforced Concrete Structures. Applied Mechanics and Materials, 2012. 166: p. 935-938.

[73] Cotsovos, D.M. and M.N. Pavlovic, Numerical investigation of concrete subjected to high rates of uniaxial tensile loading. International Journal of Impact Engineering, 2008. 35(5): p. 319-335.

[74] Georgin, J.F. and J.M. Reynouard, Modeling of structures subjected to impact: concrete behaviour under high strain rate. Cement & Concrete Composites, 2003. 25(1): p. 131-143.

[75] Abdelkareem, K.H., F.K. Abdelseed, and M.O. Sayed, THEORETICAL INVESTIGATION ON FLEXURAL PERFORMANCE OF RC BEAMS STRENGTHENED EXTERNALLY BY CFRP.

[76] Chansawat, K., et al., FE Models of GFRP and CFRP Strengthening of Reinforced Concrete beams. Advances in Civil Engineering, 2009. 2009.

[77] Kachlakev, D. and D. McCurry Jr, Simulated full scale testing of reinforced concrete beams strengthened with FRP composites: Experimental results and design model verification. Oregon Department of Transportation, Salem, Oregon, 2000.

[78] 318, A.C. Building Code Requirements for Reinforced Concrete. in ACI Journal Proceedings. 1962. ACI.

[79] Cotsovos, D.M., N.D. Stathopoulos, and C.A. Zeris, Behavior of RC Beams Subjected to High Rates of Concentrated Loading. Journal of Structural Engineering-Asce, 2008. 134(12): p. 1839-1851.

[80] Boresi, A.P., R.J. Schmidt, and O.M. Sidebottom, Advanced mechanics of materials. Vol. 5. 1993: Wiley New York.

[81] Desayi, P. and S. Krishnan. Equation for the stress-strain curve of concrete. in ACI Journal Proceedings. 1964. ACI.

[82] Schnobrich, W., Behavior of reinforced concrete structures predicted by the finite element method. Computers & Structures, 1977. 7(3): p. 365-376.

[83] Willam, K. and E. Warnke. Constitutive model for the triaxial behavior of concrete. in Proceedings, International Association for Bridge and Structural Engineering. 1975. ISMES, Bergamo, Italy.

[84] Kishi, N., H. Mikami, and T. Ando. An applicability of FE impact analysis on shear-failure-type RC beams with shear rebars. in Proceedings of the Fourth International Conference on Shock and Impact Loads on Structures. 2001.

[85] Dahmani, L., A. Khennane, and S. Kaci, Crack Identification in Reinforced Concrete Beams Using Ansys Software. Strength of Materials, 2010. 42(2): p. 232-240.

[86] Vecchio, F.J., Nonlinear finite element analysis of reinforced concrete membranes. ACI Structural Journal, 1989. 86(1).

[87] Thabet, A. and D. Haldane, Three-dimensional numerical simulation of the behaviour of standard concrete test specimens when subjected to impact loading. Computers & Structures, 2001. 79(1): p. 21-31.

[88] Wahyuni, A.S., V. Vimonsatit, and H. Nikraz, FEM modelling and analysis of reinforced concrete section with lightweight blocks infill. From Materials to Structures: Advancement through Innovation, 2012: p. 375.

[89] Okamura, H. and K. Maekawa, Nonlinear analysis and constitutive models of reinforced concrete. Gihodo, Tokyo, 1991.

[90] Zhang, X.Z., L.L. Liu, and K.D. Tang, Nonlinear Analysis of Reinforced Concrete Beam by ANSYS. Civil Engineering, Architecture and Sustainable Infrastructure Ii, Pts 1 and 2, 2013. 438-439: p. 663-666.

[91] Mindess, S., J.F. Young, and D. Darwin, Concrete. 2003.

[92] Arnesen, A., S. Sørensen, and P. Bergan, Nonlinear analysis of reinforced concrete. Computers & Structures, 1980. 12(4): p. 571-579.

[93] Thomas, J. and A. Ramaswamy. Nonlinear analysis of shear dominant prestressed concrete beams using ANSYS. in International ANSYS Conference Proceedings. 2006.

[94] Băetu, S. and I.-P. Ciongradi, Nonlinear Finite Element Analysis of Reinforced Concrete Slit Walls with Ansys (I). 2011.

[95] Băetu, S. and I. Ciongradi, Nonlinear Finite Element Analysis of Reinforced Concrete Slit Walls with ANSYS (II). Bul. Inst. Politehnic, Iaşi. LVIII (LXII). 1: p. 99-111.

[96] Mostofinejad, D. and S.B. Talaeitaba, Nonlinear Modeling of RC Beams Subjected to Torsion using the Smeared Crack Model. Proceedings of the Twelfth East Asia-Pacific Conference on Structural Engineering and Construction (Easec12), 2011. 14: p. 1447-1454.

[97] Kaw, A.K., Mechanics of composite materials. 2005: CRC press.

[98] Gibson, R.F., Principles of composite material mechanics. 2011: CRC Press.

[99] Christensen, R.M., Mechanics of composite materials. 2012: Courier Dover Publications.

[100] Alper, B., yuuml, and kkaragouml, Finite element analysis of the beam strengthened with prefabricated reinforced concrete plate. Scientific Research and Essays, 2010. 5(6): p. 533-544.

[101] Ibrahim, A.M. and H.M. Mubarak. Finite Element Modeling of Continuous Reinforced Concrete Beam with External Prestressing. in 2010 Concrete Bridge Conference: Achieving Safe, Smart & Sustainable Bridges. 2010.

[102] Jones, R.M., Mechanics of composite materials. 1998: CRC Press.

[103] Bathe, K.-J., Finite element procedures. 2006: Klaus-Jurgen Bathe.

[104] Adams, V. and A. Askenazi, Building better products with finite element analysis. 1999: OnWord Press Santa Fe, NM.

[105] Chan, H., Y. Cheung, and Y. Huang, Nonlinear modelling of reinforced concrete structures. Computers & structures, 1994. 53(5): p. 1099-1107.

[106] Bairán García, J.M., Nonlinear modelling of reinforced concrete structures. 2007.

Journal of Advanced Research in Applied Mechanics
ISSN (online): 2289-7895 | Vol. 22, No. 1. Pages 13-48, 2016

[107] Abbas, H., N.K. Gupta, and M. Alam, Nonlinear response of concrete beams and plates under impact loading. International Journal of Impact Engineering, 2004. 30(8-9): p. 1039-1053.

[108] Hemmaty, Y. Modeling of the shear force transferred between cracks in reinforced and fiber reinforced concrete structures. in Proceedings of the ANSYS Conference. 1998.

[109] Xinmin, W., ANSYS numerical analysis of engineering structures [M]. 2007, Beijing: China Communications Press.

[110] Wolanski, A.J., Flexural behavior of reinforced and prestressed concrete beams using finite element analysis. 2004, Citeseer.

[111] Zienkiewicz, O.C. and R.L. Taylor, The finite element method for solid and structural mechanics. 2005: Butterworth-heinemann.

[112] Bennegadi, M.L., Z. Sereir, and S. Amziane, 3D nonlinear finite element model for the volume optimization of a RC beam externally reinforced with a HFRP plate. Construction and Building Materials, 2013. 38: p. 1152-1160.

[113] Ozcan, D.M., et al., Experimental and finite element analysis on the steel fiber-reinforced concrete (SFRC) beams ultimate behavior. Construction and Building Materials, 2009. 23(2): p. 1064-1077.

[114] Jayajothi, P., R. Kumutha, and K. Vijai, Finite element analysis of FRP strengthened rc beams using ansys. Asian Journal of Civil Engineering (BHRC), 2013. 14(4): p. 631-642.

[115] Kachlakev, D., et al., Finite Element Modeling of Concrete Structures Strengthened with FRP Laminates. Final report, SPR, 2001. 316.

[116] Sayed, A.M., X. Wang, and Z.S. Wu, Finite element modeling of the shear capacity of RC beams strengthened with FRP sheets by considering different failure modes. Construction and Building Materials, 2014. 59: p. 169-179.

[117] Kim, Y.J., Flexural Response of Concrete Beams Prestressed with AFRP Tendons: Numerical Investigation. Journal of Composites for Construction, 2010. 14(6): p. 647-658.

[118] Abbas, A.L., Non-linear analysis of reinforced concrete beams strengthened with steel and CFRP plates. Diyala Journal of Engineering Sciences, 2010: p. 249-56.

[119] Li, W.S. and K. Wang, Nonlinear Analysis of RC Beams Strengthened with CFRP. Applied Mechanics and Materials, 2012. 166: p. 1517-1520.

[120] Saifullah, I., et al., Nonlinear analysis of RC beam for different shear reinforcement patterns by finite element analysis. International Journal of Civil & Environmental Engineering, 11 (01), 2011: p. 86-98.

[121] Zhou, J.W., et al., Nonlinear Finite Element Analysis of the Flexural Reinforced Concrete Beam Strengthened with CFRP Sheets. Civil Engineering, Architecture and Sustainable Infrastructure Ii, Pts 1 and 2, 2013. 438-439: p. 467-471.

Journal of Advanced Research in Applied Mechanics
ISSN (online): 2289-7895 | Vol. 22, No. 1. Pages 13-48, 2016

[122] Hawileh, R.A., Nonlinear finite element modeling of RC beams strengthened with NSM FRP rods. Construction and Building Materials, 2012. 27(1): p. 461-471.

[123] Godat, A., K.W. Neale, and P. Labossiere, Numerical Modeling of FRP shear-strengthened reinforced concrete beams. Journal of Composites for Construction, 2007. 11(6): p. 640-649.

[124] Ferreira, D., J. Bairan, and A. Mari, Numerical simulation of shear-strengthened RC beams. Engineering Structures, 2013. 46: p. 359-374.

[125] Gao, B., J.K. Kim, and C.K.Y. Leung, Experimental study on RC beams with FRP strips bonded with rubber modified resins. Composites Science and Technology, 2004. 64(16): p. 2557-2564.

[126] Maalej, M. and Y. Bian, Interfacial shear stress concentration in FRP- strengthened beams. Composite Structures, 2001. 54(4): p. 417-426.

[127] Rahimi, H. and A. Hutchinson, Concrete beams strengthened with externally bonded FRP plates. Journal of Composites for Construction, 2001. 5(1): p. 44-56.

[128] Fanning, P.J. and O. Kelly, Ultimate response of RC beams strengthened with CFRP plates. Journal of Composites for Construction, 2001. 5(2): p. 122-127.

[129] Quantrill, R., L. Hollaway, and A. Thorne, Experimental and analytical investigation of FRP strengthened beam response: Part I. Magazine of Concrete Research, 1996. 48(177): p. 331-342.

[130] Quantrill, R., L. Hollaway, and A. Thorne, Predictions of the maximum plate end stresses of FRP strengthened beams: Part II. Magazine of Concrete Research, 1996. 48(177): p. 343-351.

[131] David, E., et al. Use of FRP to strengthen and repair RC beams: experimental study and numerical simulations. in Proceedings of the eighth international conference on advanced composites for concrete repair. 1999.

[132] Garden, H. and L. Hollaway, A preliminary evaluation of carbon fibre reinforced polymer plates for strengthening reinforced concrete members. Proceedings of the ICE-Structures and Buildings, 1997. 122(2): p. 127-142.

[133] Saadatmanesh, H. and M.R. Ehsani, RC beams strengthened with GFRP plates. I: Experimental study. Journal of Structural Engineering, 1991. 117(11): p. 3417-3433.

[134] Nguyen, D.M., T.K. Chan, and H.K. Cheong, Brittle failure and bond development length of CFRP-concrete beams. Journal of Composites for Construction, 2001. 5(1): p. 12-17.

[135] Gao, B., J. Kim, and C. Leung. Taper ended FRP strips bonded to RC beams: experiments and FEM analysis. in FRP Composites in Civil Engineering-CICE 2004: Proceedings of the 2nd International Conference on FRP Composites in Civil Engineering-CICE 2004, 8-10 December 2004, Adelaide, Australia. 2006. Taylor & Francis.

Journal of Advanced Research in Applied Mechanics
ISSN (online): 2289-7895 | Vol. 22, No. 1. Pages 13-48, 2016

[136] Ahmed, O. and D. Van Gemert, Effect of longitudinal carbon fiber reinforced plastic laminates on shear capacity of reinforced concrete beams. ACI Special Publication, 1999. 188.

[137] Hung, C.C. and S.H. Li, Three-dimensional model for analysis of high performance fiber reinforced cement-based composites. Composites Part B-Engineering, 2013. 45(1): p. 1441-1447.